CAPE PENINSULA UNIVERSITY OF TECHNOLOGY

Department of Mechanical Engineering

CAPE PENINSULA
UNIVERSITY OF TECHNOLOGY

Finite Elements and Dynamic Hardness to Develop a Small Punch Test

Simphiwe Nqabisa

Bachelor of Technology in Mechanical Engineering

Submitted towards the Degree of

Master of Technology in Mechanical Engineering

Under Supervision of

Mr. W Kohlhöfer

CAPE TOWN, 2005

Declaration of Originality

The work described in this thesis was carried out in the Faculty of Engineering, Department of Mechanical Engineering (Bellville Campus) at the Cape Peninsula University of Technology. The work presented for this degree is my own and contains no material which has been presented for a degree at this or any other university and, to the best of my knowledge and belief, contains no copy or paraphrase of work published by another person, except where duly acknowledged in the text.

S. Nqabisa (MDipME, BTechME, PENINSULA TECKNIKON)

Cape Town, South Africa

December 2005

Acknowledgments

For the development of this thesis itself, I feel a deep sense of gratitude to:

- My supervisor, Mr. W. Kohlhöfer for his patience and continuous support when things rise and fall as they normally do in a research environment. He gave a perfect balance of technical direction and freedom in the pursuit of my research interest.
- My friend and mentor, Dr. O. Philander who shepherded this project from its early formless stage to its present form, his in-depth knowledge of continuum mechanics is highly appreciated.
- My friends N. Mbonde and A. Mtawa who are enrolled for PhD studies for proof reading and giving advices where necessary. Their help with some of the simulations and handy finite element tips now and then during this work cannot be forgotten.
- The staff at the Department of Mechanical Engineering Cape Peninsula University of Technology for providing an environment that is conducive for learning, a friendly atmosphere and technical support.
- All my friends, brothers and sisters and those who played a role or had an input directly or indirectly during the development of this thesis, I thank them from the bottom of my heart.
- My father and mother, M.A. and N.S. Nqabisa, for their devotion in the Lord and to their children, and for their constant demonstration of love that inspired me to pursue the maximization of my potential.

Finally, I would like to thank the Cape Peninsula University of Technology together with the National Research Foundation (NRF) for funding the project.

Abstract

Title of the Thesis:	Finite Elements and Dynamic Hardness to Develop a Small Punch Test
Degree Candidate:	Simphiwe Nqabisa
Degree and Year:	Master of Technology, 2005
Thesis directed by:	Mr. W Kohlhöfer

A Small Punch Test is a non-destructive technique for evaluating mechanical behaviour. The main advantage of this testing technique is the fact that material can be extracted from a component in service due to the small dimensions of the specimens. Typical test specimens cut from components are similar in size to a normal human fingernail.

The aim of this thesis is to use finite elements analysis (FEA) as well as dynamic hardness principles to develop a Small Punch Test. The obtained parameters are used as input in shape sensitivity and specimen simulation when using the finite element method (FEM). A Small Punch was constructed and retrofitted into the university's existing tensile test.

The Marc Mentat (FEA) program was used to model four different shapes of indenters for the purpose of selecting a suitable indenter to be used in the Small Punch test. A circular shape and a pyramidal shape were found to be the optimal shapes to be used for the Small Punch indenter. Hardness testing experiment was performed using an impact test to validate the finite elements results.

Experimental analysis models for two types of materials namely; aluminum and mild steel were developed and a tungsten carbide circular indenter was used during the Small Punch testing. Small Punch test and tensile test results were compared to prove that the Small Punch Test is an attractive method of evaluating mechanical behavior.

Nomenclature

There are many **symbols** or notations used for vectors, matrices and tensors. In this thesis no distinction is made in the notation if there is a physical quantity such as a vector or tensor or if it is a non-physical array of quantities that is written down in matrix form. The notation used is either vector-matrix form or index notation depending on what is most convenient. When index notation is used, *summation convention* $(a_i b_i = a_1 b_1 + a_2 b_2 + a_3 b_3)$ for tensors is used also. Symbols with special meaning, such as forces, displacement and so forth are explained when they are first presented in the text.

Scalars or tensors of zero order are written in italics, usually in lower case such as a

Vectors or tensors of rank one are written in boldface upright font, such as **v,** or in indicial notation as v_i. Usually in lower case letters. Vector components are written as

$$v = \begin{pmatrix} \mathbf{v}_1 \\ \mathbf{v}_2 \\ \mathbf{v}_3 \end{pmatrix}; \qquad v^T = (\mathbf{v}_1, \mathbf{v}_2, \mathbf{v}_3) \qquad v_i \qquad \text{and} \qquad (v_i)$$

Here, T means the transpose of the column vector, v_i means any of the three vector components and (v_i) means all the components.

Matrix form or index form are used for tensors of rank two. Either with bold face upper case letters, such as **S** or italic letter *S*. Components are (usually) written in lowercase italic letter such as *m*. Writing out the components of a matrix or a tensor is done as

$$\mathbf{M} = \begin{pmatrix} M_{11} & M_{12} & M_{13} \\ M_{21} & M_{22} & M_{23} \\ M_{31} & M_{32} & M_{33} \end{pmatrix}; \qquad \mathbf{M}^T = \begin{pmatrix} M_{11} & M_{21} & M_{31} \\ M_{12} & M_{22} & M_{32} \\ M_{13} & M_{23} & M_{33} \end{pmatrix}, \qquad m_{ij}, \quad \text{and}$$

M_{ij} and the meaning is the same as for vectors, with T for transpose, m_{ij} referring to any of the nine components and (M_{ij}) all components.

The usual **Cartesian coordinate system** $Ox_1x_2x_3$, has an orthogonal set of base vectors written with a 'hat' above the letter or an underscore underneath the letter.

$\{\hat{\mathbf{e}}_1, \hat{\mathbf{e}}_2, \hat{\mathbf{e}}_3\}$ or simply $\{\hat{\mathbf{e}}_i\}$ and $\|\hat{\mathbf{e}}_i\| = 1$

The 'hat' is used as a general symbol for a unit vector here, to emphasize that a vector is of unit length. Base vectors *not* of unit length are simply written as $\mathbf{e}_i$, with roman index. A vector in this particular case is then written in component base vector form as

$$\begin{aligned} \mathbf{v} &= v_1\hat{\mathbf{e}}_1 + v_2\hat{\mathbf{e}}_2 + v_3\hat{\mathbf{e}}_3 \\ &= v_i\hat{\mathbf{e}}_i \\ &= (v_i) \end{aligned}$$

and a matrix as

$$\begin{aligned} \mathbf{M} &= \hat{\mathbf{e}}_1 m_{11}\hat{\mathbf{e}}_1 + \hat{\mathbf{e}}_1 m_{12}\hat{\mathbf{e}}_2 + \ldots + \hat{\mathbf{e}}_3 m_{32}\hat{\mathbf{e}}_2 + \hat{\mathbf{e}}_3 m_{33}\hat{\mathbf{e}}_3 \\ &= \hat{\mathbf{e}}_i m_{ij}\hat{\mathbf{e}}_j \\ &= m_{ij}\hat{\mathbf{e}}_i\hat{\mathbf{e}}_j \\ &= (M_{ij}) \end{aligned}$$

In the last expression the *generalized tensor product or dyad product* $(\hat{\mathbf{e}}_i \otimes \hat{\mathbf{e}}_j = \hat{\mathbf{e}}_i \cdot \hat{\mathbf{e}}_j)$ of two vectors are utilized. In a rectangular Cartesian coordinate system the base vectors can be used to introduce two useful symbols. The dot product between two base vectors is

$$\hat{\mathbf{e}}_i \cdot \hat{\mathbf{e}}_j = \delta_{ij} = \begin{cases} 1 & \text{if } i = j \\ 0 & \text{if } i \neq j \end{cases}$$

where δ_{ij} is well known as the *Kronecker Delta.* The other symbol is defined by the vector-or cross-product of two base vectors which is

$$\hat{\mathbf{e}}_i \times \hat{\mathbf{e}}_j = \varepsilon_{ijk}\hat{\mathbf{e}}_k \qquad \text{where} \qquad \varepsilon_{ijk} = \begin{cases} 1 & \text{if } ijk = 1,2,3;\ 2,3,1;3,1,2 \\ -1 & \text{if } ijk = 3,2,1;\ 2,1,3;\ 1,3,2 \\ 0 & \text{if } i = j,\ i = k,\ j = k \end{cases}$$

The latter symbol (ε_{ijk}) is well known as permutation symbol. The dot and the cross products of vectors can be compactly written;

$$
\begin{aligned}
w &= \mathbf{u} \cdot \mathbf{v} \\
&= u_i \hat{\mathbf{e}}_i \cdot v_j \hat{\mathbf{e}}_j \\
&= u_i v_j \delta_{ij} \\
&= u_i v_i
\end{aligned}
\qquad \text{and} \qquad
\begin{aligned}
w &= u \times v \\
&= u_i \hat{\mathbf{e}}_i \times v_j \hat{\mathbf{e}}_j \\
&= u_i v_j \varepsilon_{ijk} \hat{\mathbf{e}}_k
\end{aligned}
$$

The components

$$
\begin{aligned}
w &= w \cdot \hat{\mathbf{e}}_l \\
&= u_i v_j \varepsilon_{ijk} \hat{\mathbf{e}}_k \cdot \hat{\mathbf{e}}_l \\
&= u_i v_j \varepsilon_{ijk} \delta_{kl} \\
&= u_i v_j \varepsilon_{ijl}
\end{aligned}
$$

Any other special notation will be clarified when it is used in the text.

Table of Contents

List of Figures

List of Tables

Chapter 1
Introduction

The work documented in this thesis consists of three interconnected parts: first a theoretical background related to the description of Hardness Testing, secondly an experimental study to compare the traditional tensile and hardness results with the proposed Small Punch test results, lastly a part including numerical computer simulation of the Small Punch experiment using the finite element method.

Almost all branches of engineering, especially those dealing with structures and machines are closely concerned with materials, the properties of which must be determined by tests. Although requisite design and fabrication procedures are listed in the appropriate specifications so that critical plant components enter service in a safe condition, nuclear power plants, chemical and petrochemical plants are subject to severe environments in which materials degenerate by time dependant degradation mechanisms, Penny (1995).

Such material degeneration leads to crack initiation and propagation and can, in severe cases, bring about rapid or catastrophic failure once the crack reaches a critical size. The structural integrity of any industrial plant is necessary to be assured that catastrophic failures can be prevented or at least minimised. To assure the structural integrity, frequent inspections for flaws are made using the procedures specified in the ASME Boiler and Pressure Vessel Code, Section XI (ASME 2001).

The use of metals in every phase of civilization relies on their ability to withstand the stresses encountered in service without breaking, plastically deforming, or weakening. No characteristic of a metal is more important than its response to applied stress. Engineers, designers and manufacturers are constantly aware that machinery, engines, tools, structures both large and small, and instruments of all kinds must be designed with the knowledge in mind of the mechanical properties of the metals they contain and the property changes that might occur in-service.

There is determined effort to discover the basic mechanisms that operate when a metal responds to a constantly applied stress and to device theories and equations that can quantitatively account for this response and predict it under all conditions that would be encountered in-service

The Small Punch testing technique is an attractive method for evaluating mechanical properties at different levels of degradation of material/component service life. The main advantage of this testing technique is the fact that material can be extracted and tested from a component while it is in service. Specimens to be tested have small dimensions and thus do not introduce damage or cause weakening of components. Upon removal of these specimens, components do not require post repair procedures such as that required with other kinds of destructive testing techniques. This makes the Small Punch test a non-destructive mechanical test, Nqabisa (2003). Typical test specimens cut from components are similar in size and thickness to a normal human fingernail. These techniques were invented in the United States of America in 1981, and explored in Japan in the early 80's. America progressed in this technology since the mid 80's and then it was introduced to Europe in the early 90's for tests on high strength steels, Foulds (1995).

When a metal responds to a constantly applied stress and an elevated temperature, a continuum damage approach is widely used to show that the governing equations can quantitatively account for this response. This would also encompass the various Finite Element Analyses to be performed.

1.1 Background Information

Over the last decades, many techniques applied on non-standard small specimens have been developed to extract a multitude of mechanical and physical properties i.e. yield strength, ultimate tensile strength, Young's Modulus, Ductility, etc. The use of small-scale techniques for mechanical testing of materials is now spreading through out the world. The Small Punch test technique (also known as the miniaturised disc bend test) is a tool for measuring mechanical characteristics of materials extracted from components during their operation, Manahan et al. (1986).

The technique has been used mainly for the determination of fracture toughness, and to the estimation of mechanical properties such as yield stress and ultimate tensile stress, Foulds et al. (1995) & Dobes et al. (2002). For this purpose Small Punch with a constant displacement rate will be developed and used.

In the field of Small Punch testing the finite element analysis (FEA) is a simulation instrument, which is widely used. The FEM is considered to be the most powerful tool because it can handle large degrees of freedom simulations with a wide range of working conditions. The simulation of a Small Punch is a complex problem. The process involves non-linear parts such as material deformation, history dependant material behaviour and contact phenomena. Accepting that the finite element analysis (FEA) is the solution of a mathematical model of structural behaviour, the implication must be that the solution is an approximated answer. One part of the simulation is the modelling of the material behaviour. This field is generally established on the principles of continuum mechanics and there are a number of constitutive models to choose from when performing a FEA. In order to get reliable results from a Small Punch simulation, one important precondition is that the material model is representative.

The development of the Small Punch test is a process involving several steps also depending on the intended use. Generally it involves construction of a specimen holder, indenter or a punch rod its holder and the specimen to be tested. Then, these components are assembled together and retrofitted on a tensile or fatigue tester. During the testing phase a specimen is indented using a high strength indenter (tungsten carbide) and a load displacement curve is deduced as an output result.

A load–displacement curve from the Small Punch test includes useful information that is related to the standard test properties such as the tensile property, fracture toughness and ductile–brittle transition temperature. Some early works have focused on obtaining empirical correlations between the transition temperatures from the Small Punch test and the fracture appearance transition temperature (FATT) or ductile–brittle transition temperature (DBTT) from the Charpy test (Bulloch, 1998; Baik et al., 1983; McNaney et al., 1991; Misawa et al., 1987; Joo et al., 1992; Saucedo-Munoz et al., 2000).

In the mid 90's Foulds et al. (1995) developed an analytical method for directly measuring the fracture toughness from the Small Punch test by calculating the local strain energy in the Small Punch specimen. But these empirical and analytical approaches for predicting the standard properties have been mostly made for the unirradiated materials while an application for the irradiated materials to predict the transition temperature shifts (TTS) by irradiation is limited.

1.2 Statement of Problem

Materials and components enter service with a safe design stress. When these materials are subjected to constant or cyclic mechanical and thermal loading, time dependant degradation of the material's yield stress occurs. Time dependant degradation weakens and deteriorates the materials yield stresses. When the yield stress degrades to a point where it becomes equal to the working stress, catastrophic failure occurs.

Japanese scientists performed degradation experiments on several high strength steels that are used in power plants, chemical and petrochemical industries. During these experiments, a material specimen were placed in a furnace and heated to some elevated temperature. The material specimen was left in the furnace at the given temperature and a tensile load was applied to it for the entire time duration of the experiment. Some of these experiments continued for up to 20 years. Test specimens were removed from the material specimens at different time intervals and mechanical testing was performed on these test specimens to determine yield stress values. A set of yield stress data points were obtained for different materials being subjected to this kind of load (thermal and mechanical)-time degradation experiment. The yield stress data points were plotted as a function of time and an example of such a graph is given in fig. 1 (yield stress-time represented by triangular points). Penny et al (2005) developed a mathematical tool to fit two functions to these yield stress data points. Their investigations provided two mathematical functions that would best fit these data points and describe the yield stress degradation phenomena observed in engineering steels. These two mathematical functions are represented by a straight-line curve and the logarithmic curve (see fig. 1.1). These two curves are on a logarithmic scale. Where these two curves meet it is hypothesised that an optimum yield stress degradation point occurs. Furthermore it is hypothesized that this optimum point represents the starting point of rapid degradation. This means that the degradation rate of a material's yield stress before it reaches the optimum point is relatively slow compared to the degradation rate after the optimum point has been reached, Penny (2005).

Fig.1.2 shows the plotted yield stress values as a function of time for an 18 Cr10NiTi stainless steel subjected to a tensile stress of 90 MPa while being kept at a constant temperature of 630°C. The two fitted mathematical functions can also be observed and as stated previously, the point at which these two fitted curves intersect represents the optimal yield stress degradation point. This example of a stress-time graph is considered to illustrate the yield stress degeneration phenomenon as a

function of static thermal and mechanical loading. The stress in the vertical axis is the yield stress of the material when it enters service. The vertical and horizontal dotted lines represent the time and yield stress respectively at this optimal point.

A study of this graph shows that when the material is just put into service, it will display minute deterioration, i.e. between 10 and 100 hours (a day to five days) deterioration is infinitesimal.

The material starts to degenerate between 100 and 1000 hours (period where optimal point is reached) and inspections for flaws and other deterioration factors can be recommended to be performed at least once a year. The recommendations are based on a simple calculation (e.g. if a tensile test is conducted after say 500 hours and a yield stress value is found to be say 80 MPa Then the testing time (500h) is subtracted from time to failure (100 000) to give the remaining life span which in this case is 11 years, Penny (2005).

Furthermore when the material's life span is between 1000 and 10 000 hours (a month to a year) it is still in a safe region and inspections for flaws should be done on a semester basis. When the life span of the material is between 10 000 and 100 000 hours inspections for flaws other deterioration factors must be done frequently on a trimester base.

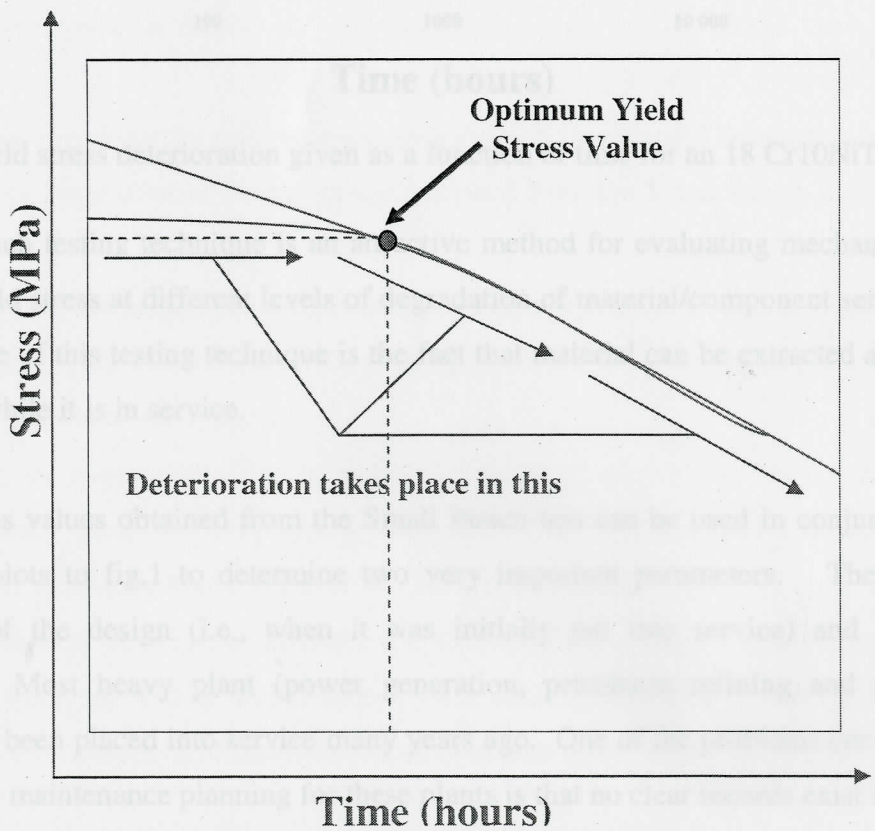

Figure 1.1: Yield stress deterioration given as a function of time for most engineering materials

These recommendations are for this particular example and are made just to demonstrate how very useful the stress time graph can be used in conjunction with the Small Punch test results to predict the remaining life of a component.

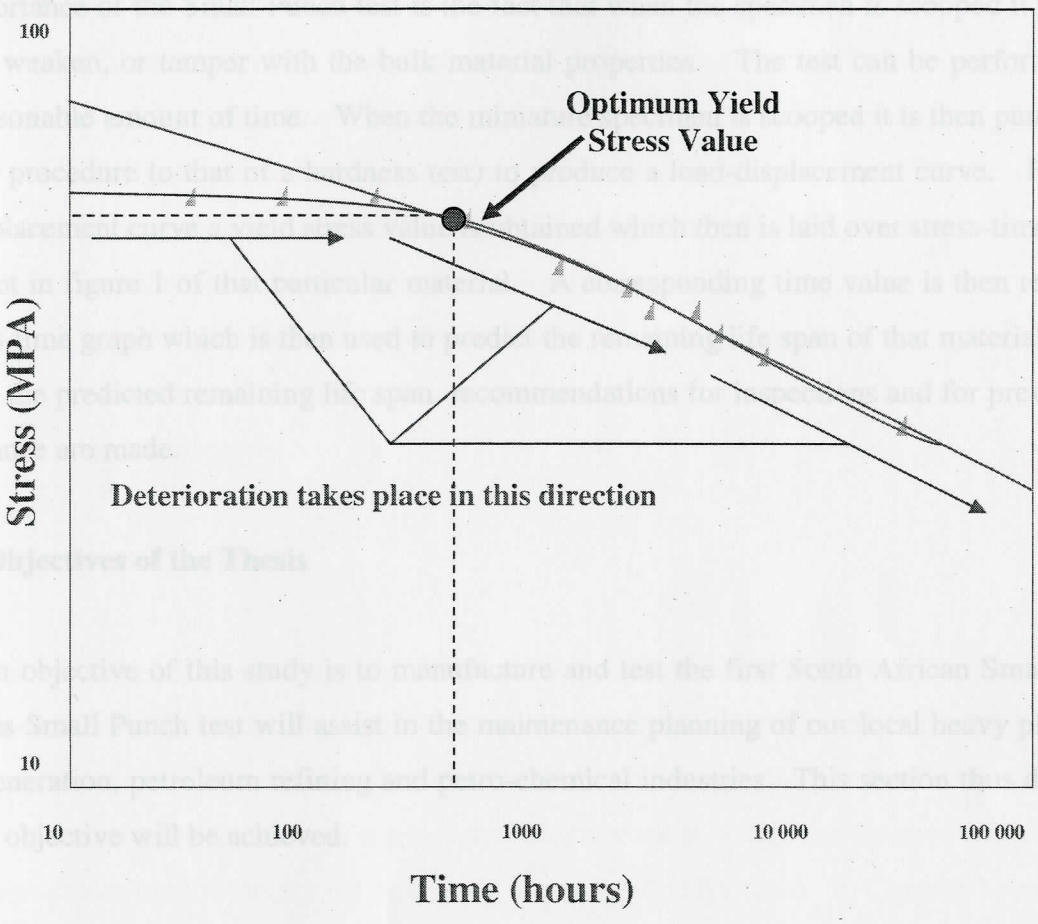

Figure 1.2: Yield stress deterioration given as a function of time for an 18 Cr10NiTi stainless steel

The Small Punch testing technique is an attractive method for evaluating mechanical properties such as the yield stress at different levels of degradation of material/component service life. The main advantage of this testing technique is the fact that material can be extracted and tested from a component while it is in service.

The yield stress values obtained from the Small Punch test can be used in conjunction with the plots similar plots to fig.1 to determine two very important parameters. These include the initialization of the design (i.e., when it was initially put into service) and remaining life expectancy. Most heavy plant (power generation, petroleum refining and petro-chemical industries) has been placed into service many years ago. One of the problems encountered today with regards to maintenance planning for these plants is that no clear records exist for their design

parameters. The yield stress obtained from the Small Punch can thus give an indication of the age of a plant and then a calculation of its life expectancy can be obtained.

The importance of the Small Punch test is the fact that when the specimen is scooped it does not damage, weaken, or tamper with the bulk material properties. The test can be performed in a short reasonable amount of time. When the miniature specimen is scooped it is then punched (in a similar procedure to that of a hardness test) to produce a load-displacement curve. From the load-displacement curve a yield stress value is obtained which then is laid over stress-time similar to the plot in figure 1 of that particular material. A corresponding time value is then read from the stress-time graph which is then used to predict the remaining life span of that material. Also, based on the predicted remaining life span, recommendations for inspections and for preventative maintenance are made.

1.3 Objectives of the Thesis

The main objective of this study is to manufacture and test the first South African Small Punch test. This Small Punch test will assist in the maintenance planning of our local heavy plant, i.e., power generation, petroleum refining and petro-chemical industries. This section thus described how this objective will be achieved.

- An initial investigation into material deterioration factors will be conducted. This should inform on current technologies being used and how the Small Punch test compares with them.
- Secondly an investigation into the working characteristics of the Small Punch test will be conducted. This will inform on the procedures to use when the manufacture and testing of Small Punch test has to occur.
- Thirdly, an investigation into an optimal indenter shape for the Small Punch test will be performed. Here we will employ the use of finite element procedures, since the cost involved with these kinds of test could be overwhelming.
- The forth step would be to manufacture the Small Punch test. Certain components of our Small Punch test will be manufactured while other components will be standard. The idea would be to retrofit the manufactured components to the tensile testing machine housed in

the Strength of Materials Laboratory in the Department of Mechanical Engineering (Bellville Campus) at the Cape Peninsula University of Technology.

- The fifth and last step would be to conduct experimental investigations into the performance of the Small Punch test.
    - The results will be presented as load-displacement curves. These results should be similar existing Small Punch test results.
    - The results should clearly indicate the yield load of material specimens tested.
    - The results obtained from these investigations should inform if our approach meets the requirements for Small Punch tests.
    - Use FEA to simulate various tester designs.
    - Furthermore the results should provide recommendations on how to improve our initial design.

1.4 Structure of the Thesis

This thesis is composed of six chapters. Chapter 1 is an introduction to the study and background information of a Small Punch Test. A literature review including principles of hardness test and application of Small Punch tests are presented in Chapter 2. In Chapter3, a process modeling and some theoretical aspects including material deformation are thoroughly discussed. Experiments and the equipment used to obtain the results are presented in Chapter 4. In Chapter 5, results and discussion of hardness and Small Punch testing are presented. In Chapter 6, conclusions and recommendations are presented.

Chapter 2
Literature Review

The following literature review gives an overview of a Small Punch testing technique its applications and limitations. As a point of departure, it starts off by defining principles of hardness testing and then the Small Punch technique to be used. These hardness principles are to be well understood as to be applied in the Small Punch test. The purpose of gaining insights to hardness principles is the fact that Small Punch operates in the same principle as the dynamic hardness. Furthermore impact hardness is used later in this work to validate FEA results.

2.1 Hardness – A Definition

Hardness is a term, which has different meanings in different situations. It may mean a resistance to penetration Davis, et al. (1964), resistance to wear Lipson, (1967) or a measure of flow O'Neill (1967). Despite the fact that these processes appear different in quality, they are all related to the plastic flow of the material.

The hardness of a material may be expressed in terms of the elastic and plastic properties of that material. This indicates that there is a relation between the hardness and the other material properties: e.g. yield strength. In this thesis hardness will be referred to as a measure of flow.

2.1.1 Scratch hardness

Mineralogists developed this type of hardness and it is the oldest form of hardness measurement, which was developed, in the early 1800's. It depends on the ability of one solid to scratch another. This method was first put on a semi scientific and experimental basis by Mohs (1822), who selected ten minerals as standards commencing with talc (scratch hardness1) and ending with diamond (scratch hardness 10). Some classical values in ascending order of hardness are given in table 2.1 below.

However, mineralogist and lapidaries broadly use the Mohs hardness scale. It is not suited for metals since its intervals are not well spaced in higher ranges of hardness. The scratching process is a complicated function of the elastic, plastic, and friction properties of surfaces that the method is not practical and does not lend to a theoretical analysis.

Table2.1: *Mohs hardness scale*

Material (Minerals)	Mohs (Hardness)	Material (Metals)	Mohs (Hardness)	Material (Miscellaneous)	Mohs (Hardness)
Talc	1	Lead	1.5	$Mg(OH)_3$	1.5
Gypsum	2	Tin, cadmium	2	Fingernail	2-2.5
Calcite	3	Aluminium	2.3-2.9	C_u2O	3.5-4
Fluorite	4	Gold, Mg, Zn	2.5	ZnO	4-4.5
Apatite	5	Silver	2.7	Mn_3O_4	5-5.5
Orthoclase	6	Antimony	3	Fe_2O_3	5.5-6
Quartz	7	Copper	3	MgO	6
Topaz	8	Iron	3.5-4.5	Mn_2O_3	6.5
Corundum	9	Nickel	3.5-5	SnO_3	6.5
Diamond	10	Chromium (soft)	4.5	Martensite	6.5-7
		Cobalt	5	MoC	7
		Rhodium	6	V_2C_3	7-8
		Osmium	7	TiC	8
		Tantalum	7		8-9
		Tungsten	7		
		Silicon	7		
		Manganese	7	Al_2O_3 (sapphire)	9
		Chromium	8	Mo_2C; SiC; VC	9-10
		Case-hardened ste	8	Boron diamond	10+

Thus, if a mineral is scratched by Orthoclase but not by Apatite, its Mohs hardness is interpolated between 5 and 6. In the determination procedure it is necessary to make sure that a scratch is actually made and not just a "chalk" mark that will rub off. If the species being tested is fine-grained or friable the test may only loosen grain without testing individual mineral surfaces. Supplements to

the mineral scale include the fingernail (2^+); a copper coin (about 3); a pocket-knife blade (5^+); window glass (5 ½); and a steel file (6 ½).

2.1.2 Static indentation hardness

This is the most commonly used method in determining the hardness of metals. This method also involves formation of a permanent indentation in the surface of the metal to be examined, the hardness being determined by the load and the size of the indentation formed. In the Brinell test (1900), Meyer (1908) the indenter consists of a hard steel ball, though in examining very hard metals the circular indenter may be made of diamond or tungsten carbide.

Another type of indenter that is used widely is the circular shape used by Ludwik (1908) and the Vickers hardness tests. Other types of indenters have been described, but they are not widely used and do not involve new principles. For this reason my discussion will be restricted to circular indenters, flat surface indenter, wedge and a pyramidal indenter. Furthermore, a finite element analysis was performed for the above-mentioned small indenters to account for the discussion. The discussion for indenter simulations will follow in chapter 4 which deals with process modelling.

The Brinell hardness test is the oldest of the hardness test and the most commonly used today for the determination of hardness for metallic material. The test is frequently used to determine the hardness of forging and the castings that have a grain structure that is too course for the Rockwell or Vickers hardness testing. However, the Brinell test is conducted on large parts of the material in question by varying the test force and the ball size. Indentation diameters must be read using a microscope. The hardness number corresponding to a particular indentation diameter is read off from a table in which load, indenter size, indentation sizes, and hardness numbers are correlated. It is often difficult to read indentation diameters accurately as sinking or piling often occur around the indentation. This test can be used on any metallic materials.

Advantages of the Brinell test

(a) One scale covers the entire hardness range although compatible results can be obtained if the ball size and test force relationship is the same.

(b) There is a wide range of test forces and ball sizes to suit every application.

The Brinell test suffers from serious disadvantages

(a) *The main weakness of this test is the need to optically measure the indent size.*

(b) *The process is very slow and the sample preparation is much slower than the actual testing*

(c) *It produces a fairly large indentation, particularly on soft materials*

(d) *It cannot be used near the edge of the specimen.*

(e) *It cannot be used on thin metals since the reactions from the test anvil might influence the test results*

However, irrespective of these limitations, it does give a linear scale of hardness and is particularly useful for my research work. It is rarely employed for production testing since it takes time, requires expensive equipment and leaves large indentations on the work.

The Vickers hardness test method consists of indenting the test material with a diamond indenter, in the form of a right pyramid with a square base and an angle 136^0 between opposite faces. The hardness number is equal to the load divided by the product of the lengths of the diagonals of the square impression. The Shore scleroscope measures hardness in terms of the elasticity of the material. A diamond-tipped hammer in a graduated glass tube is allowed to fall from a known height on the specimen to be tested, and the hardness number depends on the height to which the hammer rebounds; the harder the material, the higher the rebound. The advantages of this test are that the test is rapid, accurate, suitable for metals as 0.15mm, can be used up for values exceeding 800 Brinell, and is most suitable for determining the hardness of case-hardened or nitrated surfaces, only one type of indenter is used for all types of metals and surface treatments. The test is also thoroughly adaptable and very precise for testing the softness and hardness materials under varying loads. The main disadvantage to this test is that the Vickers machine is a floor standing machine that is more expensive than the Brinell or Rockwell machines.

Furthermore, it should be noted that the performance of this test might lead to indenters deforming. Thus, it is of particular interest to note that the indenter itself may be deformed or permanently deform in the course of the indentation process. I would have to accept that for soft metals the indenter will be deformed elastically, but for harder metals some permanent deformation may occur if this happens during the application.

2.1.3 Dynamic hardness

Dynamic hardness can be defined with static hardness as metal resistance to local indentation when a fast moving indenter produces an indentation. In practical terms/method this can simply be explained as, an indenter that is allowed to fall under gravity on to the metal surface. The indenter will rebound to a certain height and leave an indentation on the surface. It should be noticed that it is assumed that Young's modulus for the indenter metal is the same as for static conditions. This type of hardness measurement involves the dynamic deformation or indentation of the metal specimen. In this type of hardness, an indenter is dropped on the metal surface and the hardness is expressed in terms of impact energy and the remaining indentation size Martel, (1895). Shore, (1918) in his rebound scleroscope the hardness is expressed in terms of the height of rebound of indentation.

A typical example of a dynamic hardness test is the Scleroscope hardness test. This test consists of dropping a diamond tipped hammer, which falls in a glass tube under the force of its own weight from a fixed height, onto the test specimen. The test measures hardness in terms of the elasticity of the material and the hardness number depending on the height to which the hammer rebounds. The harder the material then the higher would be the rebound. Advantages of this method are its portability and the non-marking of the test surface.

2.1.4 Comparison of Static and Dynamic Hardness

The dynamic hardness of a metal is the pressure with which it resists local indentation by a fast moving indenter. Under usual experimental conditions, where the speed of impact is not too large, the dynamic yield pressure is of the same order of magnitude as the static yield pressure so that, as with static hardness is essentially a measure of the elastic limit or yield stress of the metal. The dynamic yield pressure is always greater than the static yield pressure, Tabor (1951). Dynamic hardness values determined from rebound measurements will yield values which are close to those obtained in static measurements. The dynamic hardness values of hard metals are of the order of a few percent, but with soft metals the difference may be much more marked and will increase with the velocity of impact.

2.1.5 Practical Applications of Hardness

Hardness tests have a broad field of use, although as commercial tests they are possibly used on metals than any other class of materials. The hardness tests phenomenon may be used as follows:

Similar materials may be arranged in a sequence of grades according to hardness, and a specific grade may be specified for some type of service. The degree of hardness chosen depends, on experience with materials under a given service, and not upon any fundamental implication of hardness number. It is also noted that the observed hardness number cannot be utilised directly in design or analysis as can tensile strength for example.

Hardness tests can be used for products or materials quality control. They may be utilised to determine the consistency or uniformity throughout the structure of the samples of metal or the uniformity of results of some treatment such as forming, heat treatment or alloying.

When correlation between hardness and tensile strength is well established, simple hardness tests may serve to control the uniformity of the tensile strength and to indicate whether more complete tests are justified. It should also be noted that the correlation apply only over a range of materials on which tests have previously been made; heavy reliance should not be put on extrapolations from empirical formulations, rather these empirical relations should be made with extreme caution.

In general; the idea of obtaining mechanical properties, for example, tensile strength, yield stress, percentage elongation Bröklen, (1971) and fatigue life, by a simple indentation will remain the aim of technological investigations concerned. J.A. Brinell has proved the fact that such correlations can be found when he established his empirical formula in 1900:

Tensile Strength = Constant x Brinell hardness

Up to this time, this equation has been considerable help to the expert, although it only holds for certain groups of metals.

2.2 Small Punch Sampling Technique

In the Small Punch test, a disk like specimen of ϕ 10 x 0.5 mm is scooped using a cutter (see Fig. 2.2 below) specially designed for this application. The first position (a) shows the cutter prior sampling and the second position (b) shows the cutter during sampling.

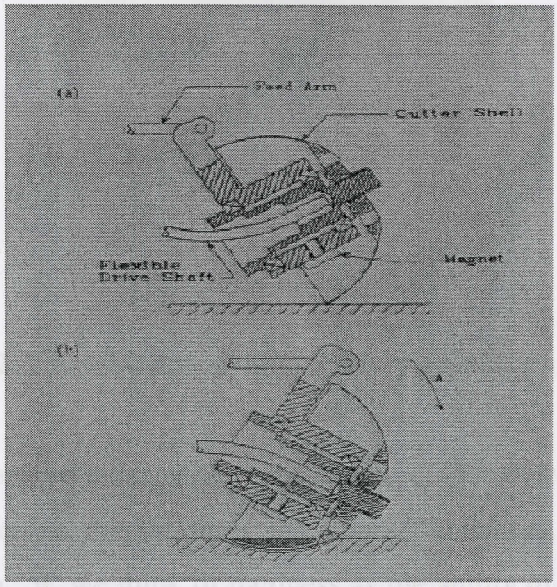

Figure 2.1: *Specimen Cutter*

In general, the sample after this specimen cutter cuts them they are ground on a horizontal surface-grinding machine. Furthermore, the sample is mechanically polished by emery paper to obtain the desired dimensions.

It is also essential to understand the indenter geometry (shape sensitivity) and hardness of the indenter itself to avoid bending or buckling of the indenter.

2.3 Theoretical Background of a Small Punch Test

The Small Punch test can simply be described as a punch and die loading test in which a small flat specimen is punched with a ball punch or an indenter (See Fig 2.2 below). In general, the Small Punch test operates in the same principles as the dynamic hardness test, but it is usually conducted under elevated temperatures more especially for fatigue or creep testing. The temperatures are usually carefully controlled through the use of an environmental chamber, a small test specimen of

about 10mm diameter and 0.5mm thickness are positioned within a specimen holder while an indenter made of tungsten carbide is positioned at the centre of the sample.

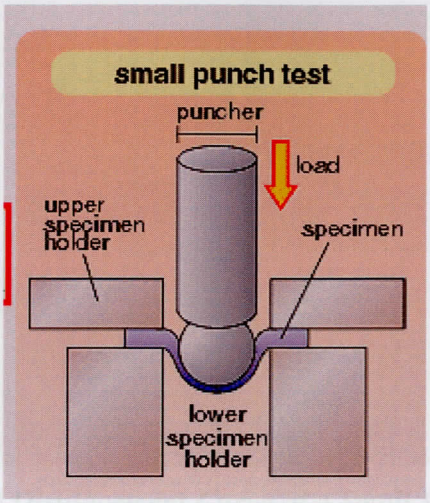

Figure 2.2: *A schematic presentation of a Small Punch Test*

The development of depth sensing indentation has allowed reliable determination of two of the most widespread mechanical properties, the Hardness and Young's modulus. In general hardness implies the resistance to deformation. If, we think of hardness as the ability of a body to resist a permanent deformation, a substance such as rubber would appear to be harder than most metals. This is because the range over which rubber can deform elastically is much larger than that of metals. The elastic properties play an essential part in the assessment of hardness for rubber-like materials.

With, metals the position is different, although the elastic moduli are large, the range over which metals deform is relatively small. Subsequently, when metals are deformed or indented, the deformation is primarily outside the elastic range and they involve considerable plastic or permanent deformation.

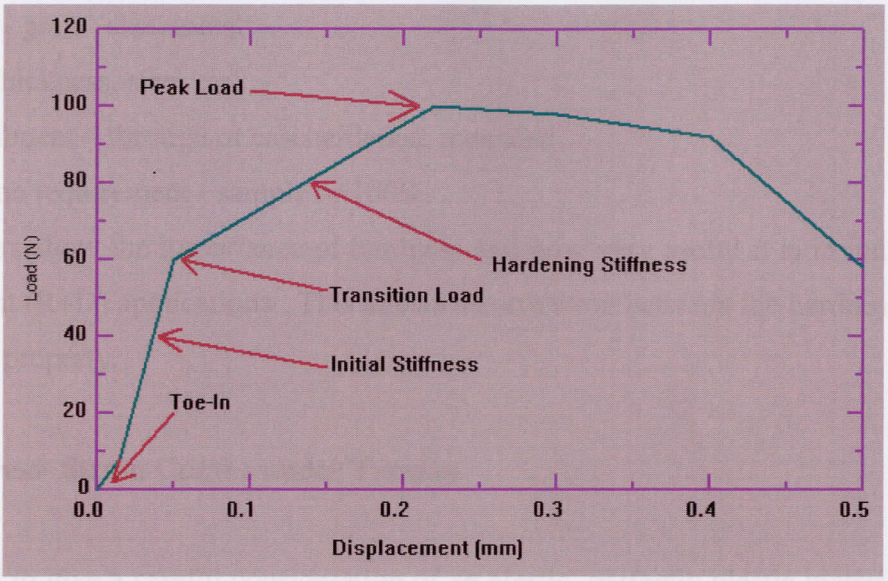

Figure 2.3: *Load Displacement Curve of a Small Punch Test results*

At first, the indenter is aligned to the centre of the specimen, and it is just allowed to touch the specimen and this stage is defined as a Toe-In (demonstrated in figure2.3 above). When the load is applied or the specimen is penetrated, it then undergoes the initial stiffness stage to the transition load. The peak load is reached at a punch displacement equal to about 50% of the initial thickness of the specimen. Then, a complete shear-through of a specimen occurs roughly at or slightly beyond a peak load. The graph goes down due to the fact that the indenter has protruded the specimen.

Hardness is now seen as the property of a material that enables it to resist plastic deformation by penetration. It can also refer to resistance to loading, scratching abrasion or cutting. Hardness is an empirical test and it is not a material property. This is due to the different hardness tests of each determines a different hardness value for the same piece of material. Hardness is used to characterize materials and to determine if they are suitable for their use. This study involves hardness testing and the use of specifically shaped indenters, which significantly harder than the test sample that is, pressed into the surface of the sample using some loading. The hardness test method has been used because it is inexpensive, easy to perform, practical and more importantly because any size or shape can be tested. Furthermore, to determine if a material has the properties necessary for its indented use. The following determining factors are used to determine the correct hardness test for an application namely,

- Approximate hardness - hardened steel, rubber etc

- Material - grain- size, metal
- Shape - thickness, size, etc
- Heat treatment – through or casehardened, annealed
- Production requirement - sample or 100%

The above factors show the importance of hardness and how very useful it is in industrial Research and Development (R+D) applications. This allows a correlation between the hardness results and the desired material property.

2.4 True Stress- Strain Curves under Tension

Firstly, it is vital to give a careful consideration of an elastic, perfectly plastic material under tension and plot the linear strain (ε) as a function of true stress (σ). The gradient of the line $O\,A$ is the ratio of stress to strain and is the Young's modulus (E) of the metal (refer to figure 2.4 below). When the load reaches a certain level, the cylinder will increase in length and this increase is non reversible. The stress at which this occurs is called the yield stress Y_0.

If the material does not work – harden, that is, if the stress remains constant during the extension, the stress strain curve is a straight line $B\,C$ and is parallel to the strain axis. If at any point D, the load is reduced, the cylinder contracts elastically along the line $D\,O'$, where this is approximately parallel to $O\,A$. If the load is completely released, the cylinder will have undergone permanent deformation $O\,O'$. On increasing the load again, the deformation will proceed elastically along $O'\,D$. and then deform plastically further along $D\,C$. Other metals, which have an unvarying, yield Y and have similar stress-strain curve as shown in figure 2.5, are called ideal plastic materials (perfectly elastic plastic). No real metals have these properties, but it is possible to obtain a close approximation to them, e.g. structural steel. In practice all metals work-harden at some stage as a result of the deformation and the stress-strain curve is of the type shown in figure2.6.

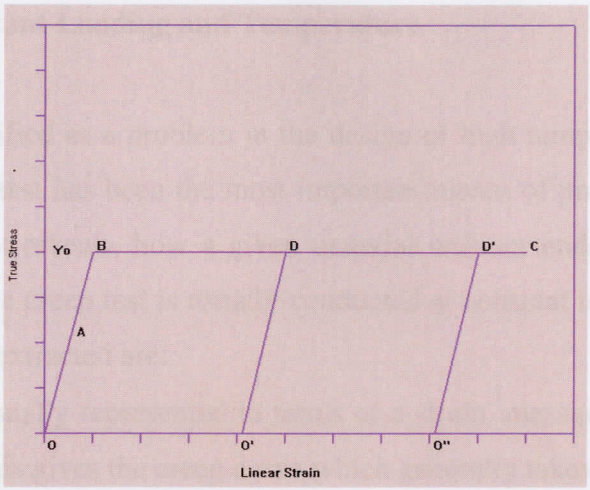

Figure2.4: *True Stress-Strain Curve*

Once plastic yielding has occurred, the stress required to produce further yielding increases rapidly at first and then gradually. Thus at any point D the stress is required to produce further plastic flow is no longer the initial yield stress Y_0 but a larger stress, so that the yield stress varies with the amount of deformation.

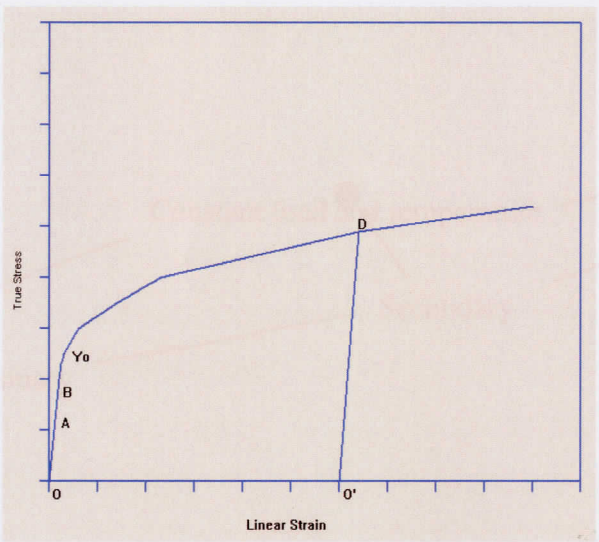

Figure 2.5: *True stress-strain curve of a metal, which work-hardens*

With many metals the dependence of yield stress Y on the strain (ε) may be approximated by the equation $Y = b\,\varepsilon^{x}$ Nadai (1931). If at point D the stress is removed, the specimen contracts elastically along $D\,O'$.

2.5 Creep under Constant Loading and Temperature

Ever since creep was identified as a problem in the design of high temperature components, the constant tensile load creep test has been the most important means of providing creep data. The data obtained from this test reveals, how a given material will act under different loading and temperature conditions. The creep test is usually conducted at constant temperature and constant load and from this the data extracted are:

- Deformation data usually represented in terms of a strain, measured over a gauge length, at various times. This gives the creep curve which generally takes the form shown in Fig. 2.6

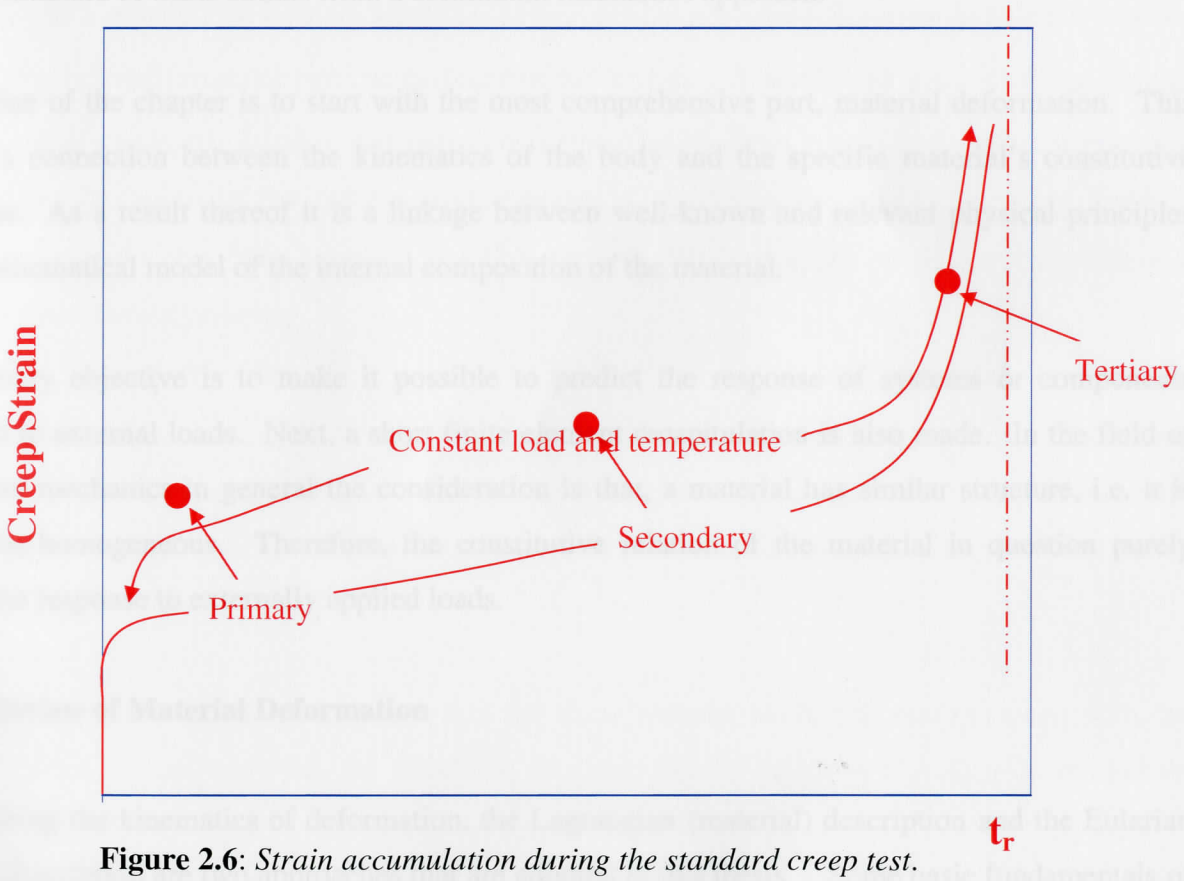

Figure 2.6: *Strain accumulation during the standard creep test.*

- Rapture data: this amount to the measurement of one coordinate - t_r the time at which rapture occurs – of the last point in figure 2.6.

Chapter 3
Process Modelling and Some Theoretical Aspects

The theory described in this chapter is purposed to serve as a background to the following chapters, especially chapter 4 and onwards. It is meant to be a short review of some of the topics in mechanical engineering and a follow up in mathematics that is necessary to have knowledge in order to get good performance from computer simulation of Small Punch. Large strains are measured during the Small Punch test in the initial configuration. The purpose of this chapter is to provide an in-depth measure of these strains from a continuum mechanics approach.

The outline of the chapter is to start with the most comprehensive part, material deformation. This topic is a connection between the kinematics of the body and the specific material's constitutive behaviour. As a result thereof it is a linkage between well-known and relevant physical principles and a mathematical model of the internal composition of the material.

The primary objective is to make it possible to predict the response of systems or components subjected to external loads. Next, a short finite element recapitulation is also made. In the field of continuum mechanics in general the consideration is that, a material has similar structure, i.e. it is said to be homogeneous. Therefore, the constitutive relation of the material in question purely defines the response to externally applied loads.

3.1 Review of Material Deformation

In describing the kinematics of deformation, the Lagrangian (material) description and the Eularian (spatial) description are two approaches that are adopted in this thesis. Some basic fundamentals of continuum mechanics pertaining to material deformation can be found in Fung (1994) the Mase brothers (1999) and Holzapfel (2001).

Lagrangian Description

In his description, Lagrange suggests that one follows the history of individual *particles*. Therefore the two variables are a particle label and time. The label, is for example, the particle position at some reference in time, i.e. the initial position **X** at $\mathbf{t = t_0}$. The assumption is then that the current position, x, of a material particle is related to the initial position for the same particle through a smooth differentiable vector valued function $\mathbf{f} : A \rightarrow B$, that is to say

$$x = \mathbf{f}(\mathbf{X}, t), \quad \text{Where, } \mathbf{f}^T = (f_1, f_2, f_3) \qquad 3.1.1$$

The initial position vector $\mathbf{X} = X_i \hat{\mathbf{e}}_i$ is the *material coordinate* of a particle and the current position vector $\mathbf{x} = x_i \hat{\mathbf{e}}_i$ is the *spatial coordinate*. The dummy index is summed over the Cartesian indexes (1, 2, 3), which means the summation convention has been used. To satisfy the continuum assumption of a material (at least in interior points) it is also necessary that there is an exact one-to-one mapping between material particle positions at two arbitrary t_0 and t_1 (or initial time and current time). In other words, the function that maps the material points from A to B must tally the points in the initial to the points in the current configuration. Conversely, the inverse mapping function should be true and it should be achieved as, $\mathbf{f}^{-1} : B \rightarrow A$ the initial position of the material point as a function of the current position.

$$\mathbf{X} = \mathbf{f}^{-1}(\mathbf{x}, t) \qquad 3.1.2$$

In principle this latter formulation is called Eularian description, where the independent variables are the current time and current position [1]. The spatial description is foremost used in fluids dynamics where the particle history is not of great importance. In solid mechanics the Lagrangian formulation is the most common in use.

It (Lagrangian) has a credible advantage that the finite element mesh will deform along with the analysed body. From now on, the functions like the one in equation (3.1.1) will be written as $\mathbf{x} = \mathbf{x}(\mathbf{X}, t)$ and we will adopt the use of Lagrange formulation only.

---

[1] Although this is the basis of the spatial description usually the function $\mathbf{f}^{-1}$ is not known. It is possible though to measure the velocity, or continuum rate of motion at a spatial point in a flow field (fluid or gas for example). We then have the velocity vector field as $\mathbf{v} = \mathbf{v}(\mathbf{x}, t)$ which then leads to the so called the material derivative in the Eularian description.

In the material description the velocity and acceleration of the particle is then written in indicial notation as

$$v_i(\mathbf{X},t)=\left.\frac{\partial x_i}{\partial t}\right|_{\mathbf{X}} \qquad \text{And} \qquad a_i(\mathbf{x},t)=\left.\frac{\partial v_i}{\partial t}\right|_{\mathbf{x}}=\left.\frac{\partial^2 x_i}{\partial t^2}\right|_{\mathbf{x}} \qquad 3.1.3$$

respectively.

In figure 3.1 below a material element Ω in a continuum body in a region in space $\Re^3$ is shown in the initial (A) and deformed, or current configuration (B) in a Cartesian frame of reference. The deformation of a body is defined by the *displacement* of every material point in the body with reference to initial or referential configuration (A in figure 3.1). The displacement is the cause of rigid-rotation, translation and deformation of material element.

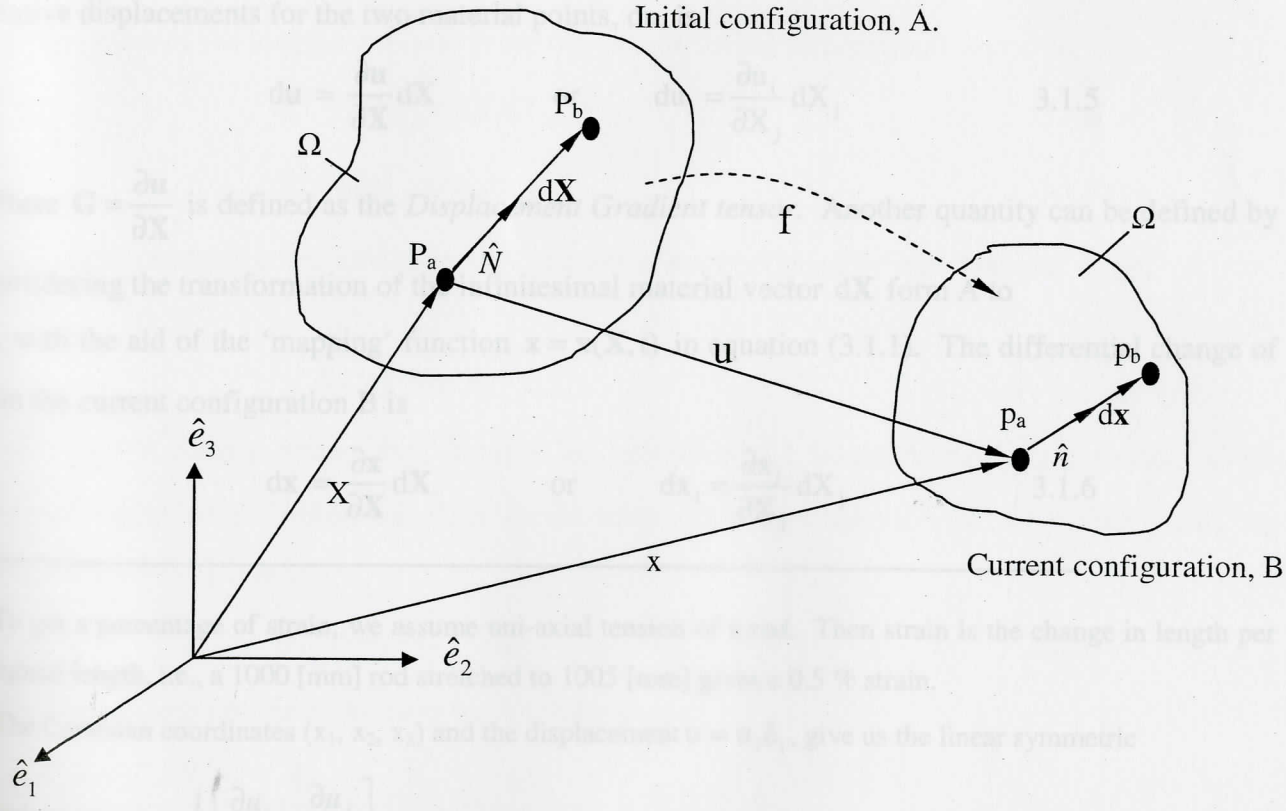

Figure3.1: *Deformation of a material element Ω in a continuum body, from initial configuration A, to current (deformed) configuration B*

In order to measure the deformation in a body the measure of strain is used [2]. The measure of strain makes it possible to do a distinction between rigid-body motion and deformation of a material element in a body. This is useful when dealing with constitutive models for a material as they describe the relation between stress (force per unit area) and strain. For small displacements a linear measure of deformation, is called the strain tensor [3]. For large displacement it implies large rigid-body motion and large deformation, and hence the linear deformation is not applicable. In the next section, a general formulation, of displacement of a continuum body is followed by presentation of relevant deformation measures and coupled stress measures that can be used in numerical analysis.

3.1.1 Summary of the Displacement

From figure 3.1 above we can define the displacement of a material point, P_a for example, from initial configuration A to current configuration B, with label p_a as

$$\mathbf{u}(\mathbf{X}) = \mathbf{x}(\mathbf{X}) - \mathbf{X}. \qquad 3.1.4$$

The time symbol t is then dropped for convenience. With material point p_b taken into account, the relative displacements for the two material points, du, is

$$d\mathbf{u} = \frac{\partial \mathbf{u}}{\partial \mathbf{X}} d\mathbf{X} \quad \text{or} \quad du_i = \frac{\partial u_i}{\partial X_j} dX_j \qquad 3.1.5$$

Where $\mathbf{G} = \frac{\partial \mathbf{u}}{\partial \mathbf{X}}$ is defined as the *Displacement Gradient tensor.* Another quantity can be defined by considering the transformation of the infinitesimal material vector $d\mathbf{X}$ form A to B, with the aid of the 'mapping' function $\mathbf{x} = \mathbf{x}(\mathbf{X}, t)$ in equation (3.1.1). The differential change of x in the current configuration B is

$$d\mathbf{x} = \frac{\partial \mathbf{x}}{\partial \mathbf{X}} d\mathbf{X} \quad \text{or} \quad dx_i = \frac{\partial x_i}{\partial X_j} dX_j \qquad 3.1.6$$

---

[2] To get a percentage of strain; we assume uni-axial tension of a rod. Then strain is the change in length per original length, i.e., a 1000 [mm] rod stretched to 1005 [mm] gives a 0.5 % strain.

[3] The Cartesian coordinates (x_1, x_2, x_3) and the displacement $\mathbf{u} = u_i \hat{e}_i$, give us the linear symmetric

Strain tensor $\varepsilon_{ij} = \frac{1}{2}\left[\frac{\partial u_i}{\partial x_j} + \frac{\partial u_j}{\partial x_i}\right]$.

and $\mathbf{F}=\frac{\partial \mathbf{x}}{\partial \mathbf{X}}$ is defined as the *Deformation Gradient tensor.* The relationship between **G** and **F** is noticeable by writing equation (3.1.4) as

$$d\mathbf{u}=\mathbf{G}d\mathbf{X}=d\mathbf{x}-d\mathbf{X} \qquad 3.1.7(A)$$

and

$$d\mathbf{x}=\mathbf{F}d\mathbf{X}=\mathbf{G}d\mathbf{X}+d\mathbf{X} \qquad 3.1.7(b)$$

so

$$\mathbf{F}=\mathbf{G}+\mathbf{I} \qquad \text{or} \qquad \mathbf{G}=\mathbf{F}-\mathbf{I} \qquad 3.1.7(c)$$

Where, **I** is the identity matrix (i.e. $\begin{pmatrix}1&0&0\\0&1&0\\0&0&1\end{pmatrix}$) consequently if **F** and **G** are known for all time t, the local deformation for each material point is also known, in principle.

F and **G** contain rigid-body rotation that does not contribute to the deformation of the continuum body. Thus, straining deforms the body and some other measure is needed. One possible alternative is to define a stretch ratio between initial and current configuration for the material vector.

Let the square of the lengths in A and B configurations for the infinitesimal vector be

$$dL^2=\|d\mathbf{X}\|^2=dX_i dX_i, \qquad 3.1.8\ (a)$$

$$dl^2=\|d\mathbf{x}\|^2=dx_j dx_j, \qquad 3.1.8\ (b)$$

respectively, and define the stretch ratio λ as current length divided by initial length. Thus,

$$\lambda=\frac{dl}{dL}=\sqrt{\frac{dx_j dx_j}{dX_i dX_i}} \qquad (3.1.9)$$

When $\lambda=1$ it simply means that, there is no stretching and therefore rigid-body motion of the material vector only. Substituting the above relationship into equation (3.1.6) it then yields the current square length to be

$$dl^2=dx_j dx_j=F_{jk}dX_k F_{jl}dX_l, \qquad 3.1.10$$

using this equation in the expression for λ it then yields

$$\lambda^2=\frac{F_{jk}dX_k F_{jl}dX_l}{dX_i dX_i}=\frac{dX_k}{\sqrt{dX_i dX_i}}F_{jk}F_{lk}\frac{dX_l}{\sqrt{dX_m dX_m}}=\hat{N}_k F_{jk}F_{kl}\hat{N}_l \qquad 3.1.11$$

Where $\hat{\mathbf{N}}$ is a unit vector in the d**X** direction. In vector-matrix notation or the so-called symbolic notation, this can be written

$$\lambda^2 = \frac{d\mathbf{X}^T}{\|d\mathbf{X}\|}\mathbf{F}^T\mathbf{F}\frac{d\mathbf{X}}{\|d\mathbf{X}\|} = \hat{\mathbf{N}}^T\mathbf{F}^T\mathbf{F}\hat{\mathbf{N}} \qquad 3.1.12$$

The use of these equations can aid and make it possible to measure the stretch ratio in any direction $\hat{\mathbf{N}}$ at any material point defined by **X** or **x.**

It order to get valuable results from the previous equation it is essential to derive principal stretch directions. The *polar decomposition theorem* states that any motion can be decomposed into pure rigid-body rotation and pure stretch in three mutual perpendicular directions. The deformation gradient tensor **F** specifies the rotation and stretch of each material line in a body between two times[4]. To decompose **F**, the point of departure is to recognise that an arbitrary material vector can be transformed from A to B (see figure 3.1) in two ways: a stretch along the principal axes followed by a rigid-body rotation of those axes, or a rigid-body rotation of the principal stretch axes followed by a stretch in those directions. The decomposition is then

$$\mathbf{F} = \mathbf{RU} = \mathbf{VR}, \qquad \text{and} \qquad \mathbf{R}^T\mathbf{R} = \mathbf{I} \qquad 3.1.13$$

Where **U** is the *right stretch tensor,* **V** the *left stretch tensor* and **R** the rigid-body *rotational matrix.* To obtain the *symmetric* tensor **U**, using the initial configuration as the basis, the square of the current length is used. From equation (3.1.10) it is

$$dl^2 = d\mathbf{x}^T d\mathbf{x} = d\mathbf{X}^T\mathbf{F}^T\mathbf{F}d\mathbf{X} = d\mathbf{X}^T\mathbf{C}d\mathbf{X}, \qquad 3.1.14$$

And $\mathbf{C} = \mathbf{F}^T\mathbf{F}$, is the *Cauchy-Green deformation tensor.* Now from the decomposition theorem

$$\mathbf{C} = (\mathbf{RU})^T\mathbf{RU} = \mathbf{U}^T\mathbf{R}^T\mathbf{RU} = \mathbf{U}^T\mathbf{U} = \mathbf{U}^2, \qquad 3.1.15$$

where the last term means every component in U squared (*symmetric matrix*). The decomposition of **C** in eigenvectors and eigenvalues leads to the sought tensor, i.e.

$$\mathbf{C} = \sum_{i=1}^{3} \bar{\lambda}^2_i \, \hat{\mathbf{N}}_i \otimes \hat{\mathbf{N}}_i \qquad 3.1.16$$

And then

$$\mathbf{U} = \sum_{i=1}^{3} \bar{\lambda}_i \, \hat{\mathbf{N}}_i \otimes \hat{\mathbf{N}}_i \qquad 3.1.17$$

Finally, from the *right* polar decomposition the above rotational matrix is

$$\mathbf{R} = \mathbf{F}\,\mathbf{U}^{-1} \qquad 3.1.18$$

[4]The path between these two times is not known and can be of importance, especially in non-isotropic materials. For the purpose of this thesis, it is possible to neglect the path.

A *left* polar decomposition using the current configuration as the basis, the square of the reference length is

$$dL^2 = d\mathbf{X}^T d\mathbf{X} = (\mathbf{F}^{-1}d\mathbf{x})^T \mathbf{F}^{-1}d\mathbf{x} = d\mathbf{x}^T(\mathbf{F}\mathbf{F}^T)^{-1}d\mathbf{x} = d\mathbf{x}^T\mathbf{B}^{-1}d\mathbf{x}, \qquad 3.1.19$$

Where $\mathbf{B} = \mathbf{F}\mathbf{F}^T$ is the F*inger deformation tensor.* The decomposition now gives

$$\mathbf{B} = \mathbf{V}\mathbf{R}(\mathbf{V}\mathbf{R})^T = \mathbf{V}\mathbf{R}\mathbf{R}^T\mathbf{V}^T = \mathbf{V}\mathbf{V}^T = \mathbf{V}^2 \qquad 3.1.20$$

Again this decomposition yields

$$\mathbf{B} = \sum_{i=1}^{3} \tilde{\lambda}_i^2 \, \hat{\mathbf{n}}_i \otimes \hat{\mathbf{n}}_i \qquad 3.1.21$$

And

$$\mathbf{V} = \sum_{i=1}^{3} \tilde{\lambda}_i \, \hat{\mathbf{n}}_i \otimes \hat{\mathbf{n}}_i \qquad 3.1.22$$

Another way of finding **U** is to use the **R** matrix, from equation (3.1.13) and from the expression for **U.**

$$\mathbf{F} = \mathbf{R}\mathbf{U} = \Rightarrow \mathbf{V} = \mathbf{R}\mathbf{U}\mathbf{R}^T = \sum_{i=1}^{3} \bar{\lambda}_i \; (\mathbf{R}\hat{\mathbf{N}}_i) \otimes (\mathbf{R}\hat{\mathbf{N}}_i) \qquad 3.1.23$$

Take note, from the above equations the following relationship is valid: $\bar{\lambda}_i = \tilde{\lambda}_i$ and $\hat{\mathbf{n}}_i = \mathbf{R}\hat{\mathbf{N}}_i$, which shows that the order of rotation and stretch are irrelevant. In the previous results in equation (3.1.12) If $\hat{N}_i$ are principal directions then the principal stretches can be obtained as

$$\lambda_i^2 = \left(\frac{dl_i}{dL_i}\right)^2 = \hat{\mathbf{N}}_i^T \mathbf{U}^2 \hat{\mathbf{N}}_i \qquad \text{or} \qquad \lambda_i = \frac{dl_i}{dL_i} = \mathbf{U}_i, \qquad 3.1.24$$

And index i is the principal direction for **U** the dL_i and dl_i are the initial and current lengths of a material vector in the principal direction i. Therefore, a measure of the stretching of a material line in three mutual orthogonal directions is obtained. It should be noted that this measure tells nothing about the path between initial and deformed configuration.

3.1.2 A Summary of Strain

As a point of departure, a one-dimensional description of strain is made and thereafter a more general approach is made using the theory from the previous section.

One-dimensional strain

In essence, a measure of deformation is already obtained with the stretch ratio. It can be used in some situations to quantify deformation i.e. measure of strain. As mentioned in our discussion earlier on that, $\lambda = 1.0$ means no straining. For the materials (metals) that will be used to perform experiments in the contents of the next chapter 4, it is not adequate. A typical structural steel can have a strain of 1.001 (or 0.1%) at yield and to use the stretch ratio, as a measure does not give sufficient resolution in the results. Instead the measure of strain is used with zero strain when λ has a value one (1). In one dimension, along an arbitrary material vector d**X**, the strain is defined as the function of the stretch ratio λ that is,

$$\varepsilon = f(\lambda) \qquad 3.1.25$$

The function f is subjected to some chosen constraints, and they can be derived using a mathematical tool called: Tailor series expansion and f to be considered around the unstrained state. Tailor series can be expanded to the desired number of terms but we will show only the first four terms to demonstrate the beauty of mathematics.

$$\varepsilon = f(1) + (\lambda - 1)\frac{df}{d\lambda} + \frac{1}{2!}(\lambda - 1)^2 \frac{d^2 f}{d\lambda^2} + \frac{1}{3!}(\lambda - 1)^3 \frac{d^3 f}{d\lambda^3} + \bullet\bullet\bullet \qquad 3.1.26$$

The series motivates the choice of f (1) = 0 to get ε to be zero at $\lambda = 1$. For small strains, when second order and higher terms are ignored, the well-known definition of one-dimensional strain should be achieved, i.e., if $\frac{df}{d\lambda} = 1$ for $\lambda = 1$ this is the case. Also, to get the exponential increased strain with increased stretch the choice can be $\frac{d^2 f}{d\lambda^2} > 0$ for $\lambda > 0$ this gives positive strain in tension. These moderate restrictions give many possibilities to choose a 'strain function'. A commonly used measure in plasticity, which is also relevant here, is the logarithmic or true strain

$$f(\lambda) = \ln\lambda \quad \text{or} \quad \varepsilon_{true} = \varepsilon^{\ln} = \ln\lambda \qquad 3.1.27$$

Considering the standard uniaxial tensile test, the strain is defined as

$$d\varepsilon_{true} = \frac{dl}{l} \qquad 3.1.28$$

Where l is the current specimen length. The definition is infinitesimal because l is constantly changing during the test. Integrating the above equation (3.1.28) from the initial configuration (C_1) to deformed configuration (C_2), therefore from initial length L to final length l, it gives the true strain of the specimen. i.e.

$$\varepsilon_{true} = \int_{C_1}^{c_2} d\varepsilon_{true} = \int_{L}^{l} \frac{dl}{l} = \ln \frac{l}{L} \qquad 2.1.29$$

I am aware of the fact that it is not so easy to generalise a total strain measure to general deformation. However the path dependence of a material element makes it necessary to follow the deformation continuum events of each element through a large strain path. It is essential to relate an incremental strain measure to the total strain, obviously obeying the rate laws. In the one-dimensional tensile test case, where the path is completely specified, this is possible with equation (3.1.29).

Strain Considered in General Deformation

In a general case, strain can now be deduced from the polar decomposition of **F** derived from the previous above equations. A robust two-point *approximation* of a likely path dependent deformation or material strain is followed. The true strain of a material vector (or material line) oriented in $\hat{\mathbf{N}}_i$ direction (from equation 3.1.24) can be written as

$$\varepsilon^{ln} = \ln \frac{li}{Li} = \ln \lambda_i \qquad 3.1.30$$

This is in correspondence with the one-dimensional case. Using the initial configuration as a basis we can now construct a matrix, which defines a strain for a material point.

Assuming that $\varepsilon_i = f(\lambda_i)$ is the strain[5] in the principal directions given by equation (3.1.17) [6]. Then the strain tensor is

$$\varepsilon = \sum_{i=1}^{3} \varepsilon_i \, \hat{N}_i \otimes \hat{N}_i \qquad 3.1.31$$

The above equation can be used to calculate the eigenvectors and eigenvalues of $\mathbf{F}^T\mathbf{F}$ for each material point in every step of an algorithm using this measure. From equations (3.1.8 a) and (3.1.8 b) we can now derive a change in length (square) equation of a material vector from initial to deformed state.

$$dl^2 - dL^2 = d\mathbf{X}^T (\mathbf{F}^T\mathbf{F} - \mathbf{I})\, d\mathbf{X} = d\mathbf{x}^T (\mathbf{I} - (\mathbf{F}^T\mathbf{F})^{-1})\, d\mathbf{x}, \qquad 3.1.32$$

[5]To keep the generality no function is chosen. This means therefore, strain is the function of the stretch ratio in a principal direction given by $\mathbf{F}^T\mathbf{F}$.

[6]The stretch ratios are identical to the eigenvalues in this equation.

Where, $\mathbf{E}=\frac{1}{2}(\mathbf{F}^{T}\mathbf{F}-\mathbf{I})$ is the *Green-Langrage strain tensor* and $\mathbf{e}=\frac{1}{2}(\mathbf{I}-(\mathbf{F}^{T}\mathbf{F})^{-1})$ is the *Almansi strain tensor.* In these formulae the strain is obtained directly from the deformation gradient without the need of calculating the principal directions.

It has been mentioned earlier on that, the relevant measure of strain in metal plasticity is the logarithmic or true strain. Therefore in linear deformation (using two point approximations) the strain tensor is

$$\boldsymbol{\varepsilon}^{\ln}=\sum_{i=1}^{3}\ln\bar{\lambda}_{i}\,\hat{\mathbf{N}}_{i}\otimes\hat{\mathbf{N}}_{i}=\ln\mathbf{U} \qquad 3.1.33$$

and i refer to the principal values and directions of **U.**

Strain rate

A definition of strain rate is necessary, in order to cope with the path-dependence of the material, which simply means that, the constitutive relations must be in rate form.

From equation (3.1.13) the velocity of the material particle is defined as

$$\mathbf{v}(\mathbf{X},t)=\left.\frac{\partial\mathbf{x}(\mathbf{X},t)}{\partial t}\right|_{\mathbf{x}}, \qquad 3.1.34$$

and the deferential velocity between two adjacent particles in the current configuration (B in figure 3.1) is

$$d\mathbf{v}=\frac{\partial\mathbf{v}}{\partial\mathbf{x}}d\mathbf{x}=\frac{\partial\mathbf{v}}{\partial\mathbf{X}}\frac{\partial\mathbf{X}}{\partial\mathbf{x}}d\mathbf{x}=\mathbf{L}d\mathbf{x}=\mathbf{L}\mathbf{F}d\mathbf{X} \quad \text{or} \qquad 3.1.35$$

$$d\mathbf{v}=d\dot{\mathbf{x}}=\frac{\partial}{\partial t}(\mathbf{F}d\mathbf{X})=(\dot{\mathbf{F}}d\mathbf{X}) \qquad 3.1.3$$

Where the dot ('$\bullet$') means the material time derivative $\frac{\partial}{\partial t}$, and $\dot{\mathbf{F}}=\frac{\partial\mathbf{v}}{\partial\mathbf{X}}$ and where $\mathbf{L}=\frac{\partial\mathbf{v}}{\partial\mathbf{X}}$ is the *velocity gradient.* Now the equation above yields the following

$$\mathbf{L}=\dot{\mathbf{F}}\mathbf{F}^{-1} \qquad 3.1.37$$

And considering the polar decomposition theorem, **L** consists of a rate of deformation part and a rate of rotation part. As a result it is possible to decompose **L** into strain rate, the *deformation velocity tensor;*

$$\mathbf{D}=\frac{1}{2}(\mathbf{L}+\mathbf{L}^{T}) \qquad 3.1.38$$

And the skew symmetric spin tensor

$$\boldsymbol{\Omega} = \frac{1}{2}(\mathbf{L} - \mathbf{L}^T) \qquad 3.1.39$$

Finally, if the strain rate is **D**, then an increment of strain is defined as

$$d\boldsymbol{\varepsilon} = \mathbf{D}dt = \frac{1}{2}(\mathbf{L} + \mathbf{L}^T)dt \qquad \text{or in component form, } d\varepsilon_{ij} = \frac{1}{2}\left(\frac{\partial(v_i dt)}{\partial x_j} + \frac{\partial(v_j dt)}{\partial x_i}\right) \qquad 3.1.40$$

and an incremental strain measure is obtained. The total strain is then

$$\varepsilon_{ij} = \int_{t1}^{t2} d\varepsilon_{ij} = \int_{t1}^{t2} D_{ij}\, dt \qquad 3.1.41$$

which is the three-dimensional extension of the logarithmic strain. There are some limitations to the above formulation. If it is possible to follow the material point through the deformation and evaluate the integral at a time (t), then the quantity will be meaningful. Another serious considerable restriction is that either the principal strain axes do not rotate during the deformation or they follow the rigid body motion. To put it more robustly, the material deformation must be consistent with the geometrically defined deformation. The deformation velocity tensor is not an adequate strain measure for the overall deformation because it describes only the current deformation. The total deformation can be obtained with rate form of the Green-Lagrange strain tensor $\dot{\mathbf{E}}$. This tensor is related to **D** as

$$\dot{\mathbf{E}} = \mathbf{F}^T\mathbf{D}\mathbf{F} \qquad 3.1.42$$

And it must be integrated to give a total strain measure.

3.2 An Overview of Stress

The conventional concept of stress suggests that when designing for working loads, component dimensions and forces need to be related in order to decide on suitable operating stress values. In this summary, the basic forms of stresses are discussed in relation to external factors (forces) and internal stresses and strains. These relationships are crucial for an insight into component behaviour.

It is interesting to note that stress is not a physical or measurable parameter but only a mathematical tool relating loading to geometry. On the other hand, strain is a physical measure. It is also interesting to note that in general deformation however; there is number of stress measures available, just as for strain. Therefore, the stress and the strain measures must be *work-conjugate* which means

that an increment of strain multiplied by the current stress must be a valid infinitesimal increment of work per unit volume of material. From a material point of view, and possibly the most important measure of stress from an engineering perspective is the *Cauchy stress.* This is a direct measure of traction per unit area of any internal surface in the body, i.e. force per unit area. The Cauchy stress tensor is given as

$$\sigma = \begin{pmatrix} \sigma_{11} & \sigma_{12} & \sigma_{13} \\ \sigma_{21} & \sigma_{22} & \sigma_{23} \\ \sigma_{31} & \sigma_{32} & \sigma_{33} \end{pmatrix} \qquad 3.1.43$$

and it is a Eularian measure, with all variables defined at an instance in time. The current force *da* in the current configuration is then

$$\mathbf{df} = \boldsymbol{\sigma}\mathbf{da} = \boldsymbol{\sigma}\,\hat{\mathbf{n}}\,\mathrm{da} \qquad 3.1.43$$

Then, the complementary strain to use with this stress is the deformation velocity tensor, i.e. the power P per unit current volume is

$$\mathrm{P} = \boldsymbol{\sigma} : \mathbf{D} \qquad 3.1.44$$

and the increment of work derived from the increment of strain, $\mathrm{d}\boldsymbol{\varepsilon} = \mathbf{D}\mathrm{dt}$ is

$$\mathrm{dW} = \boldsymbol{\sigma} : \mathbf{D}\mathrm{dt} = \boldsymbol{\sigma} : \mathrm{d}\boldsymbol{\varepsilon} \qquad 3.1.45$$

The colon (':') means the inner product of two matrices, i.e. the component of the matrices is multiplied and the products are summed. The incremental work derived in (3.1.45) can be written in component form or the well-known indicial notation as, $\mathrm{dW} = \sigma\mathrm{ij}\mathrm{Dij}$.

Considering changes of a body from an initial or undeformed configuration to a current configuration a Lagrange concept must be used because strain is normally measured from the former state. A stress measure formulated with the material description is the *second Piola-Kirchoff stress tensor* **S.** It transforms the current force **df**, back to the initial state $\mathbf{df}_0$, and is related to an area element in the initial state $\mathbf{da}_0$.

$$\mathrm{d}\,\mathbf{f}_0 = \mathbf{S}\,\mathrm{d}\mathbf{a}_0 = \mathbf{S}\,\hat{\mathbf{N}}\mathrm{da}_0 \qquad 3.1.46$$

Where $\mathbf{df} = \mathbf{F}\mathbf{df}_0$ and **F** is a deformation gradient tensor. Previously we have defined the rate of Lagrangian strain, $\dot{\mathbf{E}}$ which relate the work-conjugate strain measure to the stress measure. Now, the power (P) per unit *initial* volume is

$$\mathbf{P} = \mathbf{S} : \dot{\mathbf{E}} \qquad 3.1.47$$

and the increment of work is, $\mathrm{d}\mathbf{E} = \dot{\mathbf{E}}\mathrm{dt}$

$$\mathrm{dW} = \mathbf{S} : \mathrm{d}\mathbf{E} \qquad 3.1.48$$

Using the non-vanishing Jacobean (J), this transforms stress from one measure to the other. Now let $J = \det \mathbf{F} = \frac{dV}{dV_0}$ where V and V_0 are material's volumes in current and referential configurations respectively. Then the relations can be written as

$$\mathbf{S} = J\,\mathbf{F}^{-1}\boldsymbol{\sigma}\left(\mathbf{F}^{-1}\right)^{T} \qquad \text{Or} \qquad \boldsymbol{\sigma} = J^{-1}\mathbf{F}\mathbf{S}\mathbf{F}^{T} \qquad 3.1.49$$

The strain and stress measures that are mentioned here are commonly used in engineering, but there are other mechanical complementary variable that can be found in reference literature.

3.3 Finite Element Method

In this segment some basic information about non-linear finite element theory is given. Most of the equations listed in this section are given without prior derivation. The topic is very broad and the theory, or information given, in this section is based primarily on Logan (1993), Bathe (1982), Zienkiewics (1994) and the Nastran Patran manuals.

The general idea behind the finite element method (FEM) is to build a mathematical model of a structure, based on a series of discrete finite elements, where each element has a mathematically defined relationship between force (load) and displacement. These relationships are assembled to a global stiffness matrix, for the analysed structure. Upon applying homogeneous boundary conditions, a matrix solution scheme can be utilised to determine a structural response to the applied loads. For static stress problems this can be formulated in general terms as $\mathbf{F} = \mathbf{K}\mathbf{U}$ where a vector of forces ($\mathbf{F}$) is related to a displacement vector $\mathbf{U}$ via the global stiffness matrix $\mathbf{K}$.

In non-linear problems, the stiffness matrix $\mathbf{K}$ is not assumed to be constant as opposed to linear problems, hence it is presumed to incorporate geometrical material, and load stiffness terms. In order to solve these non-linear problems, the prescribed loading or displacement is applied in incremental stages, and an iterative mathematical solution scheme is used to find equilibrium at each increment. It should be noted that if the non-linear changes (become non-smooth) in the stiffness terms during the iteration process, the solution may diverge or may not converge at all.

To find the response of a solid body subjected to loading, some knowledge of the equilibrium conditions may be required. For any volume of the body the force and moment equilibrium must be maintained for all times. Substituting this with a less involving condition; that the equilibrium

should be maintained in average, over a finite number of elements of the body is the bases of the displacement finite element method. In principle the equilibrium statement is usually formulated in the form of virtual work, a form that is suitable for the discrete finite element formulation.

3.3.1 Virtual Work

For a volume V with surface S in the current (deformed) configuration representing a part (element) of a body, the virtual work statement (in a rate form suitable for finite element formulation) can be written as

$$\int_v \sigma_{ij}\delta D_{ij}\, dV = \int_s t_i \delta v_i\, dS + \int_v f_i \delta v_i\, dV \qquad 3.3.1.1$$

Where δD_{ij} is the virtual rate of deformation (virtual strain rate), δv_i is the virtual velocity, t_i is the force per unit current area (surface force) and f_i are the forces per unit current volume (body forces). Hence, the internal rate of work is equal to the work of the applied force in the virtual velocity field. To formulate the discrete system of equations in the reference configuration, the left hand side of the virtual work expression can be written in reference variables. The work-conjugate stress-strain (Cauchy stress and rate deformation tensor) with the internal rate of virtual work in the reference configuration is

$$\int_v \sigma_{ij}\delta D_{ij}\, dV = \int_{v_0} J\,\sigma_{ij}\delta D_{ij}\, dV_0 \ , \qquad 3.3.1.2$$

Where $J\sigma_{ij}$ is complementary to D_{ij} in the reference configuration and J is the *Jacobean* defined earlier on.

3.3.2 Fundamental Equations of Finite Element

In general the element displacement function is **u**, and it is given by

$$\mathbf{u} = \mathbf{N}^N U^N \qquad 3.3.2.1$$

Where $\mathbf{N}^N$ are basis function or vector interpolation function and U^N are nodal displacements, and also N = 1, 2...to the number of variables present (for example the number of nodes in an element) [7].

[7] The summation convention is used on the nodal variables, indicated with uppercase superscripts.

Equation 3.3.2.1 is a kinematics constraint, and this constraint also bounds the virtual displacement field, so the virtual variation is

$$\delta \mathbf{v} = \mathbf{N}^N v^N \qquad 3.3.2.2$$

and the continuum virtual work formulation, equations (3.3.2.1) and (3.3.2.2) is discretized. The virtual rate of strain $\delta \mathbf{D}$ is associated with δv (see, for example, equation (3.3.11)) and with the assumption (3.3.2.1) it can be formulated [8] as

$$\delta \mathbf{D} = \mathbf{\Phi}^N v^N \qquad \text{Where } \mathbf{\Phi}^N = \mathbf{\Phi}^N(\mathbf{x}, \mathbf{N}^N) \qquad 3.3.2.3$$

In the above formulation the approximation of the virtual work is

$$\delta v^N \left[\int_{V_0} \Phi_{ij} \sigma_{ij} \, dV_0 - \int_S t_i N_i^N dS - \int_V f_i N_i^N dV \right] = 0 \qquad 3.3.2.4$$

Where the quantities inside the square brackets form a non-linear system of equilibrium equations.

3.3.3 Solution Method

The system of equations above, expressed more precisely as a force equilibrium is,

$$F^N(u^M) = 0 \qquad 3.3.3.1$$

and the solution can be found using various mathematics techniques, like Newton method etc. In equation (3.5.7) F^N in the conjugate component force to the N^{th} variable in the equations and the value of the M^{th} variable is u^M. The solution procedure is incremental, and in each increment the iterative Newton method solution scheme is used to find an approximation to the equilibrium equations.

3.4 A Summary of Metal Plasticity

A *constitutive model* stands for a mathematical model that describes our ideas of the behaviour of material Desai (1984) and Hill (1985). In this summary some topics in metal plasticity are described. Plasticity is also known as the *flow stress theory* and the formulation is such that the current infinitesimal strain increments (see previous section on strain) are dependant on the stresses.

---

[8] The actual formulation is: $\delta \mathbf{D}_{ij} = \frac{1}{2}\left(\frac{\partial N_i^N}{\partial x_j} + \frac{\partial N_j^N}{\partial x_i} \right) \delta \mathbf{V}^N = \mathbf{\Phi}_{ij}^N \delta \mathbf{v}^N$

The initial response of a metal to loading is elastically, i.e. the deformation is fully recoverable. If the load goes beyond the yield point, the deformation cannot be recovered. For small elastic strains, which is common in metals, the strain increment can be separated into an elastic portion and a plastic portion by using that L from section 3.1.2 can be written $L \approx L^{el} + L^{pl}$. The particular law for metals, used in the numerical simulations later on this work, is described here.

Incremental plasticity is usually formulated in three related terms. The first one is a *yield surface:* which simply means to extrapolate the concept of load at yield, and to make it possible to determine when a material responds purely elastic. The second one is a *flow rule:* which describes the plastic deformation of a material point. The final one is an *evolution law* which defines the hardening [9] of a material. A thorough review of the topics mentioned here can be found in Desai (1984), Hill (1985) and others.

The material to be used in the experiments is to be assumed to follow some idealizing criteria. As a result thereof, the following assumptions must follow: the material is isotropic, which means therefore that, the material properties are the same in all three mutual perpendicular axes, which is reasonable for mild steel. There are no environmental chambers or temperature dependence, that is to say, standard room temperature will be assumed.

The hardening behaviour is isotropic and the strain rate independent. No Bauschinger effect will be considered, which simply means that after initial loading, no unloading followed by reloading will be introduced. That is to say the magnitude of the yield stress is the same in tension and in compression. Mild steel is like other ductile materials, it exhibits large inelastic strain, and it yields at stress values lower than the material's elastic modulus (E) which is also well known as the Young's modulus. The implication is that relevant stress strain variables are the Cauchy stress and logarithmic (plastic) strain.

---

9. Hardening means how the yield and flow definitions change with plastic deformation.

Chapter 4
Experiments

The main objectives of the experimental work described here were to record the response of a normal mild steel specimen subjected to a tensile, hardness and in a Small Punch experiment. Some basic fundamental principles pertaining to the properties and testing of materials can be found in Harmer et al (1982) and Patricia, (1993). In these paragraphs these concepts will be mentioned as a preamble or an introductory statement. The *mechanical properties* of an engineering material are those that deal with the material response under applied loads. It is imperative to recapitulate that these properties are often related to stress and strain. *Material testing* is basically a research area that covers procedures and methods to determine and measure mechanical properties in the most approximated and reliable way.

There are primarily two quantities, mentioned above, that are used in the scope of the experiment[1] presented in this chapter. The first one is *stress* or the determination of the applied force or load on the tested material. The second quantity is *strain* or the change in specimen geometry as a result of the applied load. The basic mechanical property that is most crucial for the experiment described here is *plasticity* or the ability of a material to deform beyond the elastic range, namely, permanent deformation without rupture.

Materials testing is purposed to simulate the working conditions of a material and because of the large number of applications for a material there is no one 'overall-test' to perform. Alternatively tests are categorised mainly according to conditions regarding see table 4.1 below.

[1] The terms experimentation and testing are considered to have the same meaning in this thesis. Although, materials' *testing involves* both, they are closely related but not identical. The main difference is the aim to perform one or the other. Experiment, is to gather information when the outcome is uncertain. Test, is to follow standard procedures and only record the necessary information Timing (1998).

Table 4.1: *Test categories*

Load Application	**Material Specimen Conditions**	**Environmental Conditions**
The kind of stress induced	1. Form	Temperature
The rate of stress propagation	2. Dimension	Atmospheric pressure
The number of load cycles	----------	----------

The details given in table above are some examples of classification factors, but there are more than this. There are various loading conditions that are possible but the ones used in this experiment are tension and compression. Regarding the rate of load application, this experiment is classified as a dynamic test, where the load is applied at the rate where it is possible to disregard inertial effects on the test results. Also, the test is carried out at room temperature and normal atmospheric pressures as it has been mentioned previously. The main focus is on the basic quantities which are stress and strain although it is not an easy task to measure them directly. Hence we measure the load acting on a specimen in combination with the displacement of the specimen due to the applied load, and then we convert these two parameters into stress and strain.

4.1 Equipment

The testing equipment used in this experiment were a Tensile Test Hounsfield see figure 4.1 and a specimen holder and steel indenter of own construction and a tungsten carbide indenter. The tensile test consists of a frame with a bottom fixed member and a movable crosshead with the load cell attached to it. The load cell used in this experiment is registered 50 kN. In the bottom cross member a servo-actuator system with 250 kN dynamic capacity is mounted.

All measurements were made with built in sensors. The applied load was measured with the load cell, and the stretch with the displacement transducer located inside the frame. The test frame is controlled, monitored and programmed a M300 microprocessor unit, remotely accessed through an ordinary PC and tensile test in-house software. The analog to digital to digital (A/D) conversion of measurement signals is made with a resolution 240 VAC, 50/60 Hz, 530 VA of input range which means a precision of 48 VAC in the conversion.

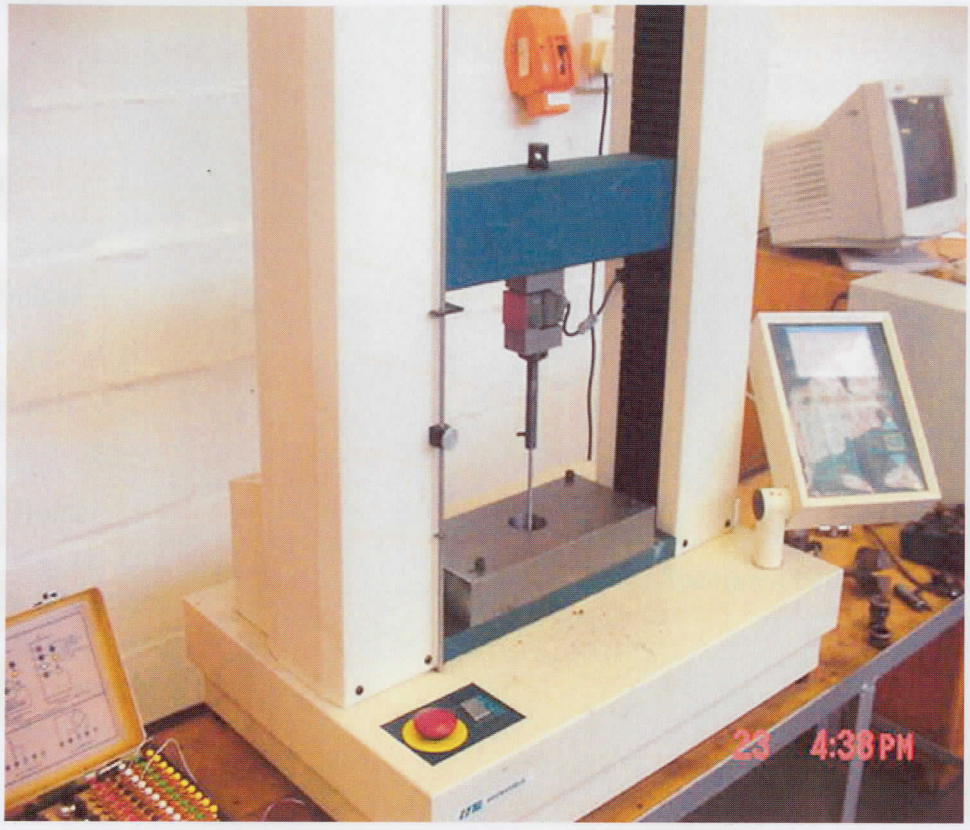

Figure 4.1: *Hounsfield tensile test used in the experiments.*

4.2 The Specimens

The specimens were made from two different materials, namely aluminium and mild steel. For further material data see appendix A. Ten samples were taken out from each of the plates, each with dimensions, thickness (T) 3[mm], width (W) 20[mm] and a length of 40 [mm]. The specimens were not prepared in any special way after they were cut from the plates and the cuts were made only in one direction. Small test specimen with the above mentioned dimensions were positioned within a specimen holder while an indenter made of tungsten carbide is positioned at the centre of the sample.

4.3 Experimental Set up

The material test was mainly conducted according to SABS (South African standard), which correspond to ISO 7438 (International standard). The following description is valid for each of the twenty specimens from the two plates. A specimen was placed in the specimen holder according to figure 4.2 and the punch was lowered to nearly contact before punching started. Next, the punch moves downward at a rate of 0.5 [$mm.s^{-1}$]. After that, the punch pause (four

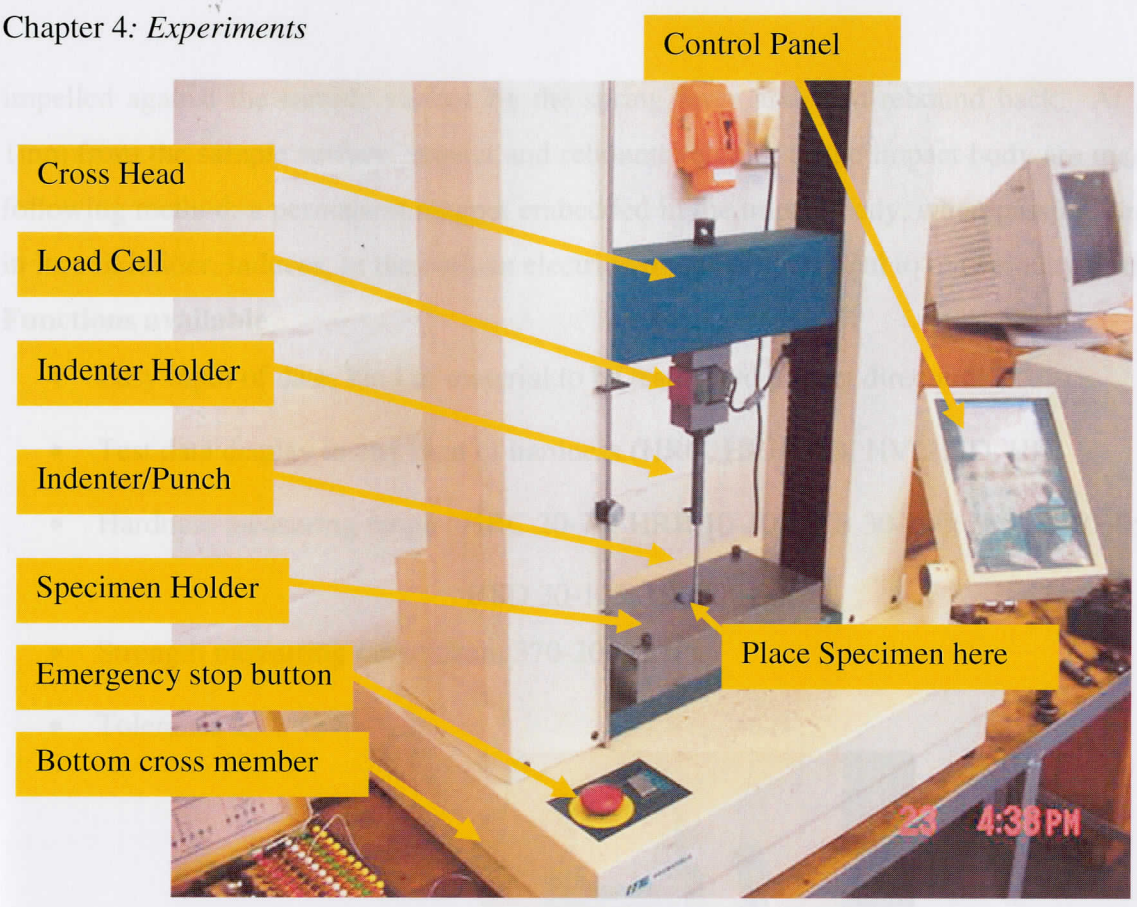

Figure 4.2: *Hounsfield tensile test used in the experiments.*

seconds) when it sheared through in the lowest positions, approximately 3.1 mm below the starting position, followed by a movement in the up direction at a rate of 1 [$mm.s^{-1}$]. During this punching procedure the punch force F^P and the punch displacement U^P were continuously monitored and recorded.

Hardness Testing Equipment

A portable ROCKLY HLN-11A (see figure 4.3) has been used in this work for the purpose of comparing various hardness values. ROCKLY HLN-11A is an advanced hand held hardness tester, characterised by its high accuracy, wide range and simplicity for operation. It is suitable for testing the hardness of all metals and widely applied in many industrial fields. The instrument is capable of converting the hardness into strength parameter automatically.

Measuring Method

The measuring method is defined as quotient of the impact body's rebound velocity over its impact velocity, multiplied by 1000. An impact body with a circular tip made of tungsten carbide is

impelled against the sample surface by the spring force and then rebound back. At a distance of 1mm from the sample surface, impact and rebound velocity of the impact body are measured by the following method: a permanent magnet embedded in the impact body, when passing through the coil in its coil holder, induces, in the coil, an electric voltage proportional to the velocity of the magnet.

Functions available

- Easy input of date, kind of material to be tested and impact direction
- Test data display in any kind of hardness (HRC, HRB, HB, HV, HSD, HL)
- Hardness measuring range : HRC 20-70; HRB 10-100; HB 30-700; HV 80-1030;

  HSD 30-105; HL 200-900
- Strength measuring range :from 370-2000 MPa
- Tolerance ±0.8 %

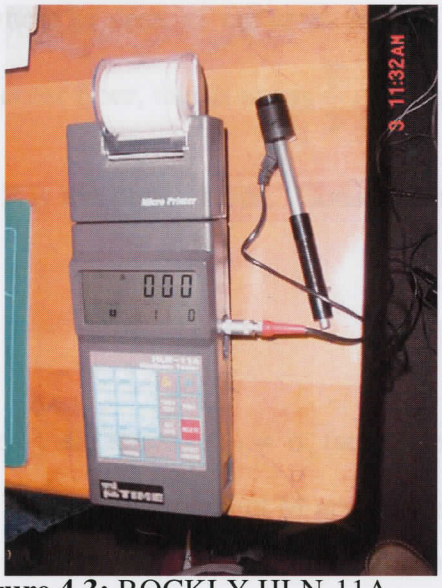

Figure 4.3: ROCKLY HLN-11A

Likewise the specimens were made from two different materials, namely aluminium and mild steel. . Ten samples were taken out from each of the plates, each with dimensions, thickness (T) 3[mm], width (W) 20[mm] and a length of 40 [mm]. The specimens were not prepared in any special way after they were cut from the plates and the cuts were made only in one direction.

4.4 Expected Material Behaviour

Because of the ductility of the tested materials, no rupture of the specimen was expected. As long as the compressive stress in the sample is lower than the yield stress, σ_y the force displacement curve

should resemble a straight line or it should be linear. When the bending moment acting on the sample has reached a sufficient magnitude (with maximum in the midsection, below the indenter) the entire midsection is strained into the plastic range of the material hence stressed beyond the yield stress and the force-displacement curve becomes non-linear. This should be evident from the force displacement curve, with a 'point' on the plot where deviation from linearity occurs.

Under the assumption that the yield stress is equal magnitude in tension and in compression, we can calculate an approximated value of the punch force needed to reach the yield stress and the shear through of the specimen. From beam theory Tonge (1972) and with the dimension given under the specimen section we can estimate the maximum bending moment, M_y, to initiate the yield as,

$$M_y = \sigma_y \frac{I}{y} = \sigma_y \frac{WT^3}{12}\frac{1}{y} = \sigma_y \frac{WT^2}{6}$$

In this instance, I is the second moment of area, of the cross section of the specimen and y is the distance from the neutral axis to the outer fiber, that is to say $\frac{T}{2}$. The elastic bending moment acting on the specimen is $M = \frac{FD}{4}$, where F is the punch force. Consequently, we get the punch force to initiate yield

$$F_y = \sigma_y \frac{2}{3}\frac{WT^2}{D}$$

And we use the value of the tabulated yield stress, $R_{eH} = \sigma_y$ (see appendix A) then $F_y \approx 25\,kN$. As yielding penetrates the cross-section the bending moment M approaches the fully plastic moment M_p which for an elastic perfectly plastic material of the same or similar cross-section as our specimens is

$$M_p = \sigma_y \frac{WT^2}{4}$$

Replacing σ_y with tabular value, like with the one above, and solving for punch force we get $F_P \approx 28\,kN$ when there is fully developed plastic behaviour in the material. But because the real material is not perfectly plastic, and a hardening behaviour is expected, the output from the experiments is expected to deviate from the values calculated here.

Tensile Test Data

The first set is standard tensile test data (see appendix A) recalculated to get the flow stress and the equivalent strain from nine points of the nominal stress-strain curve. The true values used to sketch the true stress and strain curve in (appendix A) have been achieved by using the well known relationships

$$\sigma_{true} = \sigma_{nom}(1+\varepsilon_{nom}); \qquad \varepsilon^{pl} = \ln(1+\varepsilon_{nom}) - \frac{\sigma_{true}}{E}$$

Where σ_{true} is the 'true' stress or (Cauchy stress) which we just named it a flow stress, and ε^{pl} is the logarithmic or 'true' plastic strain. The second set is the linear approximation of the plastic behaviour. The equivalent plastic strain ε^{pl}, was set in nine point, ranging from 0% to 120% strain and backward biased towards the lower values. The corresponding flow σ_f stress is then calculated from the initial values by using the least squares criteria. See appendix A for strain values that were read from a data file (in order to satisfy C++ code).

Chapter 5

Results and Discussions

The results presented in this chapter follow the outline of the thesis. First some experimental results of hardness values, FEA and the Small Punch testing are shown. Thereafter a comparison of material parameters from a tensile test (see appendix A) and the optimised parameter is made, followed by some standard output from FEA with the different material parameter set.

5.1 Experimental Results and Discussions

5.1.1 Hardness Values

Figure 5.1 below shows a comparison between the various hardness values. HRB, HRC, and HVN are Hardness Rockwell B-scale, Hardness Rockwell C-scale, and Hardness Vickers Number respectively.

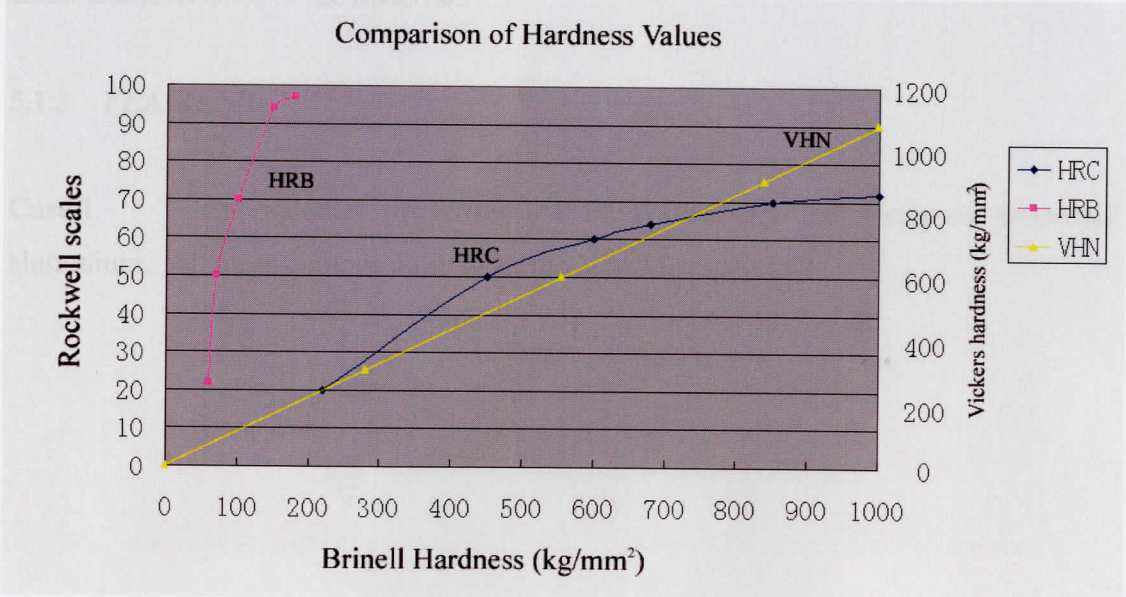

Figure 5.1: *Hardness numbers as a function of Brinell hardness. Tungsten carbide ball used above 500 kg/mm²*

5.1.2 Discussion of the Hardness Results

Circular and Pyramidal indenters (both Vickers and Rockwell) produce plastic flow at the tip of the indenter at very light loads. The circular indenter is indicated by the magenta line which is HRB on the graph. The Pyramidal is shown by navy blue line which is HRC on the graph. The flat surface indenter is shown by a yellowish colour. These results are quite significant and they validate the FEA results.

This is due to the fact that the tip is infinitesimal. Thus the hardness number obtained from these tests has the single value over a wide range of loads. This fact makes Vickers and Rockwell very convenient to use as careful load constraints are not critical.

For circular indenters (Brinell) this is not the case. The yield pressure increases with the size of indentation. This is due to the fact that the indentation changes shape as it varies in size. Thus, the yield pressure increases with the load. These tests are easy to perform, and thus the Brinell test, using the analysis of Meyer, may be used to examine the stress-strain characteristics of the material.

5.1.3 FEA Results

Case 1 The indenter properties are mild steel and the specimen properties are aluminium. All these contour plots show the Von Mises stresses.

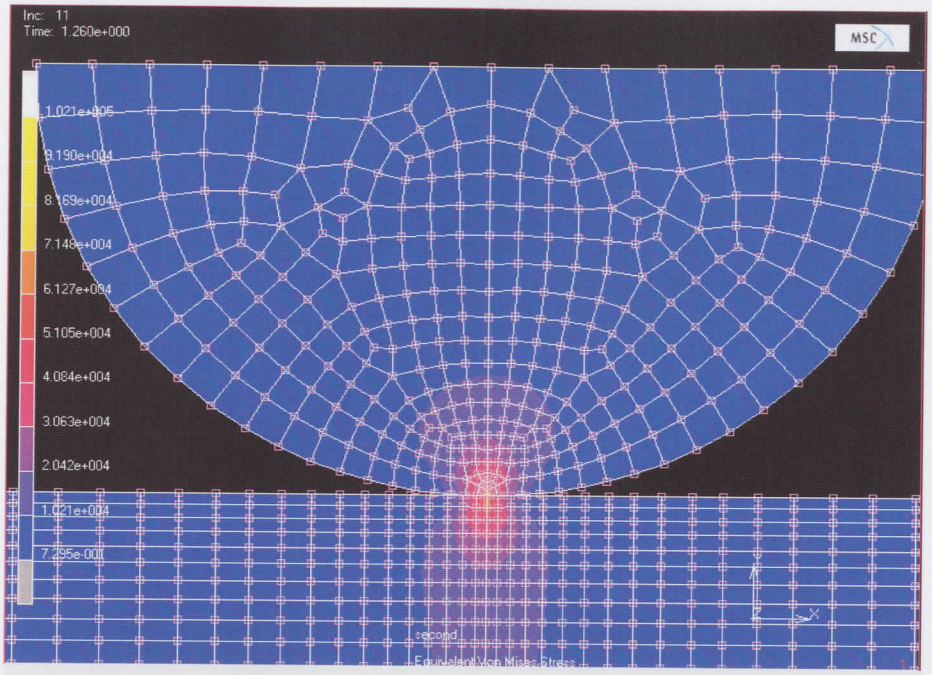

Figure 5.2: *Circular Indenter Analysis*

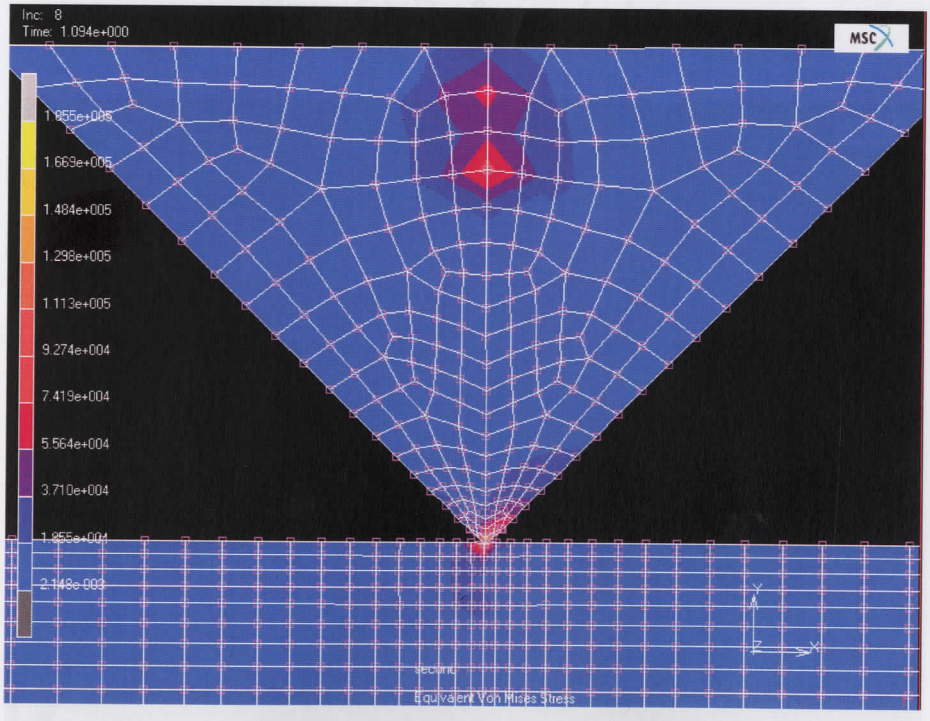

Figure 5.3: *Pyramidal Analysis*

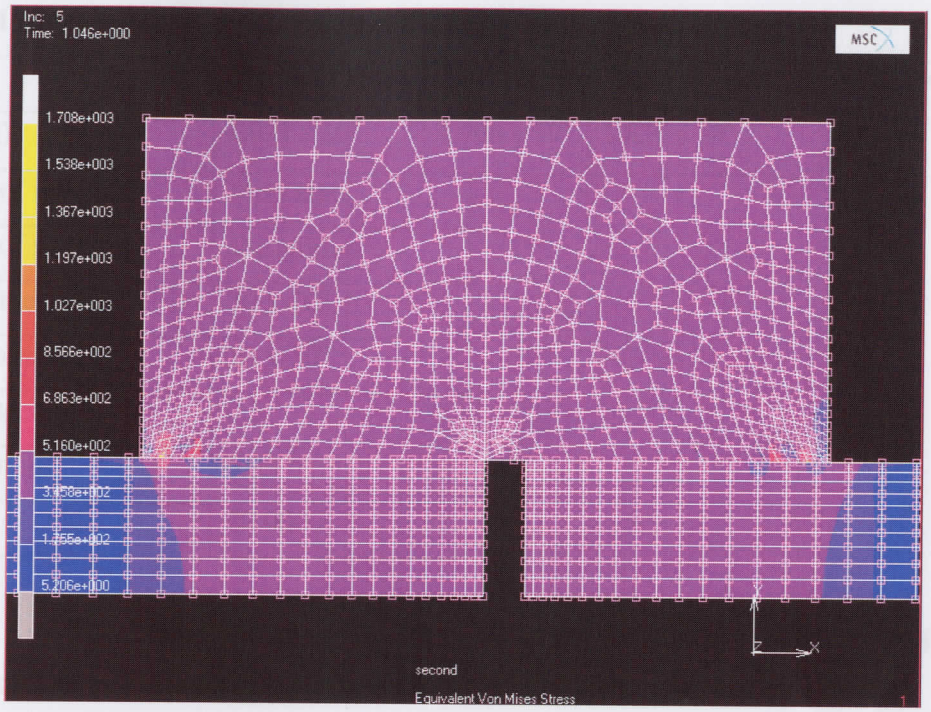

Figure 5.4: *Flat Surface Analysis*

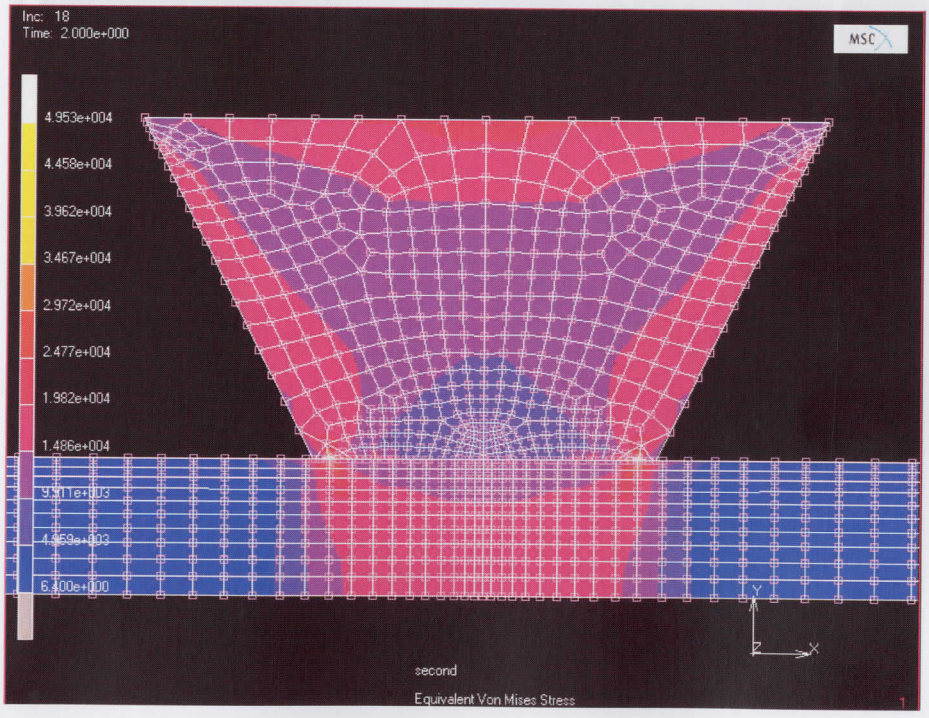

Figure 5.5: *Wedge Surface Analysis*

Table 5.1 a: *Showing the stresses induced and material characteristics*

	Circular indenter	Flat indenter	Pyramidal indenter	Wedge indenter
σ_{max} (PSI)	**1.021×10^5**	**1.708×10^3**	**1.855×10^5**	**4.963×10^4**
Material of indenter	Mild steel			
Material of specimen	aluminium			
E (mild steel) PSI	30×10^6			
E (aluminium) PSI	10×10^6			
υ (mild steel)	0.3			
υ (aluminium)	0.33			
P (PSI)	20 000			

Case 2: The following analyses were performed using the indenter properties of tungsten carbide and the specimen has been considered to be engineering steel.

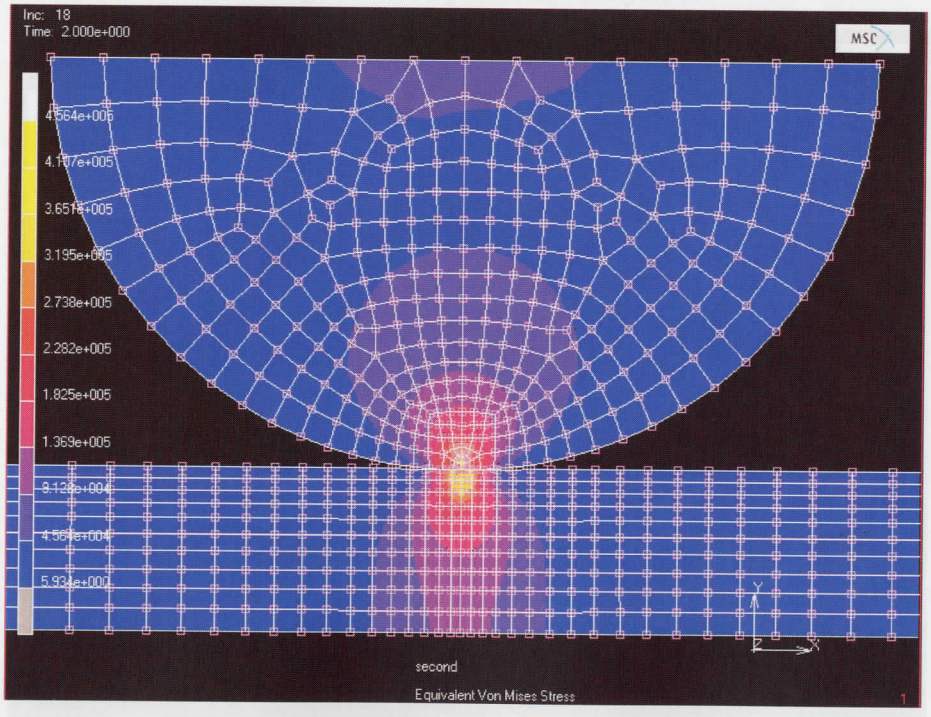

Figure 5.6: *Circular Punch Analysis*

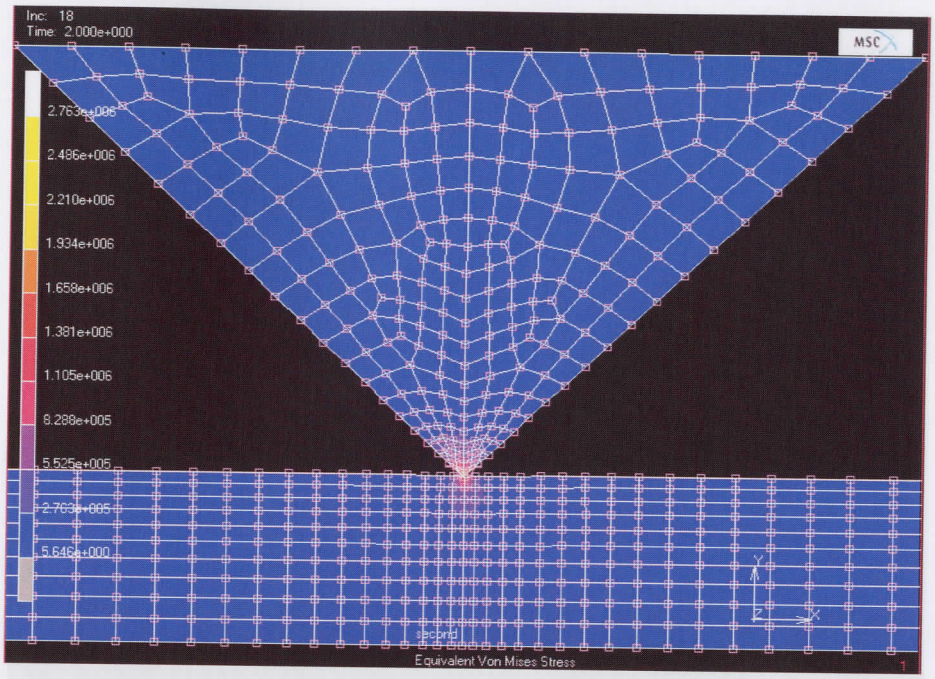

Figure 5.7: *Pyramidal Analysis*

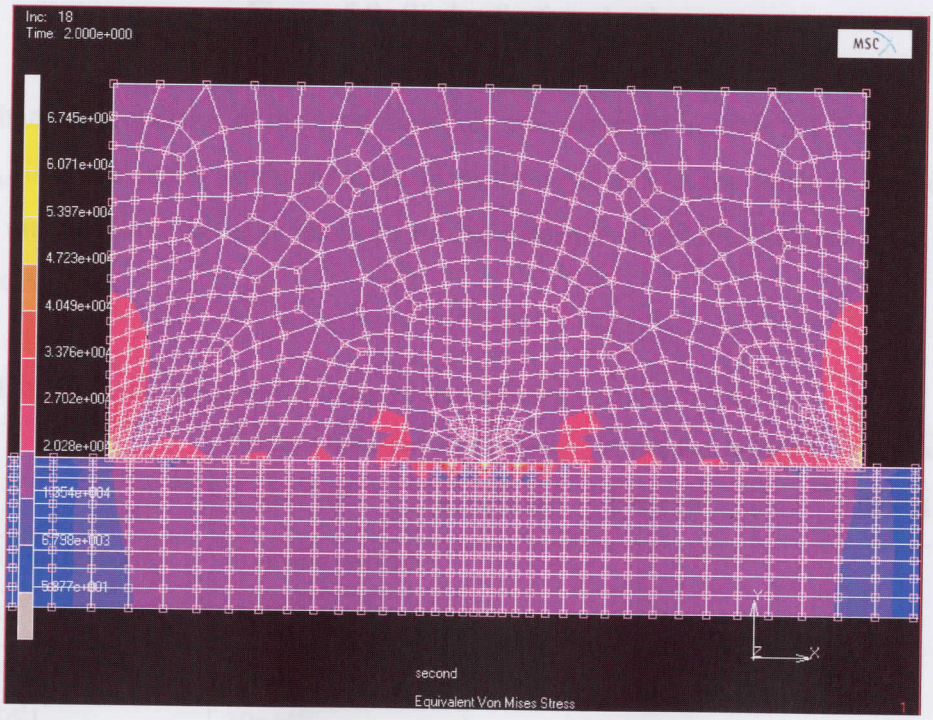

Figure 5.8: *Flat Surface Analysis*

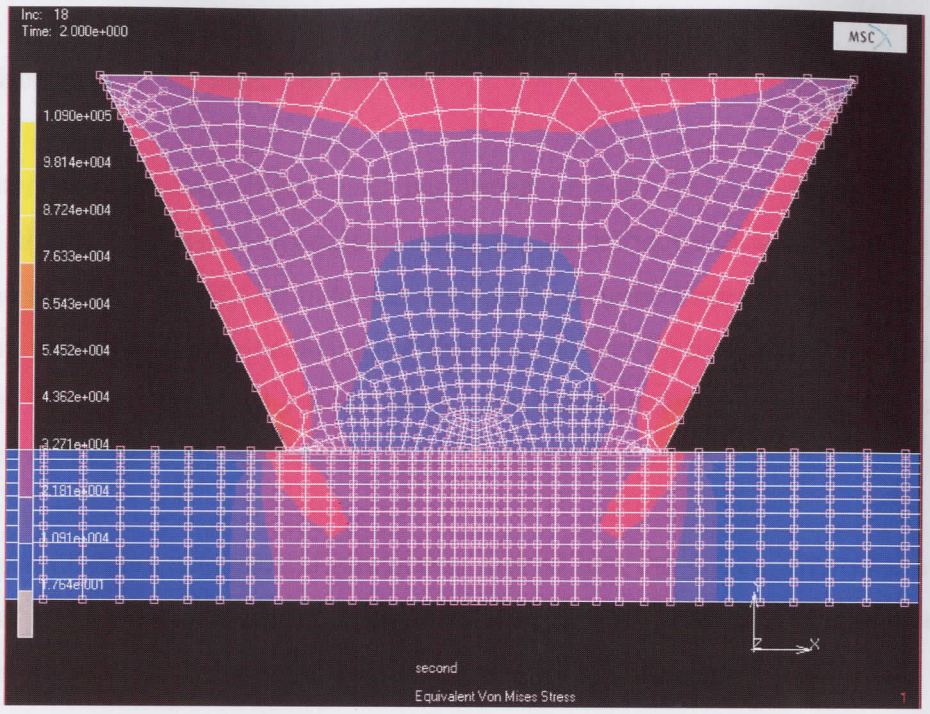

Figure 5.9: *Wedge Surface Analysis*

The mechanical properties of the used materials are presented in table 5.1 b below. In these table σ_{max} is a maximum stress obtained from the results, ν is the Poisson's ratio E is the Young's modulus and the edge pressure P. An example of an FEA output file is shown in Appendix B.

Table 5.1 b: *Showing the stresses induced and material characteristics*

	Circular indenter	**Flat indenter**	**Pyramidal indenter**	**Wedge indenter**
σ_{max} (PSI)	**4.564×10^5**	**6.745×10^4**	**2.76×10^6**	**1.090×10^5**
Material of indenter	tungsten carbide			
Material of specimen	steel			
E (tungsten carbide) PSI	92×10^6			
E (steel) PSI	30×10^6			
υ (tungsten carbide)	0.26			
υ (steel)	0.3			
P (PSI)	20 000			

5.1.4 **Discussion of the FEA Test Results**

A computer numerical simulation was performed on four different shapes of indenters, namely, a circular indenter, a pyramidal indenter, a flat surface and wedge surface indenter. The elastic behaviour of all four indenters is considered to be isotropic. All non-linearity's, induced by the elasto-plastic behaviour of the material and by the contact with friction, are assumed to be negligible small Tabor (1951). The indenters that are used in this simulation are defined by Tabor as circular, flat surface, Wedge surface and pyramidal.

The purpose of doing a numerical simulation looked into the deformation of the indenter, 'strain-less' indentation effects and effectively validated the results. The analyses together with the experiments support a mathematical model in order to explain the results.

The Finite Element Analysis (FEA) is a type of elasticity solution because it approximately satisfies the mechanical governing equations. The problem is formulated in terms of load and displacement degrees of freedom, so that the compatibility and stress distribution equations are satisfied. All these effects give a description of the plastic deformation and yielding of a metal under a uniform tension or compression when the metal (indenter) is pressed against the specimen. The results show that the stresses are not really simple tensile or compressive stresses but they are set up in various directions under the indenter.

The maximum stress values exhibits that, for the circular and the pyramidal shapes the maximum stresses occur at the tips of the indenters. This can be clearly seen on the steel vs. aluminium Von Mises contour plots above where maximum stresses are distributed around the indenter tips and these maximum stresses are 1.021×10^5 and 1.885×10^5 for the circular and the pyramidal indenters respectively. For the tungsten carbide vs. steel the maximum the stresses are 4.564×10^5 and 2.76×10^6 for the circular and the pyramidal indenters respectively.

The maximum stresses of flat surface and wedge indenters are 1.708×10^3 and 4.963×10^4 for steel vs. aluminium. Similarly the maximum stresses of flat surface and wedge indenters are 6.745×10^4 and 1.090×10^5 for tungsten carbide vs. steel. These maximum stresses occur at the edges of the indenters for the flat surface and the wedge indenters. This implies that in general for these two types of indenters the edge pressure has to be increased quite significantly in order to cause yielding. Thus this makes consideration for plastic flow under combined stresses.

In all the FE models discussed here the edge load was applied gradually. The hardness test which was performed applied impact load. Therefore energy transferred to the specimen was considered when these FEA results were validated. Furthermore, load-displacement curves below were plotted using the FEA results. These load-displacement curves were plotted on strategic nodal points of contact between the indenter and the specimen. The purpose of these FEA load-displacements curve is to compare them with those of the Small Punch test. The circular indenter proves to be feasible in both cases shown below. For both of these cases the displacement is in proportion to the load applied (see fig. 5.10 & fig.5. 14)

Case 1 Load displacement curves of a mild steel indenter and an aluminium specimen

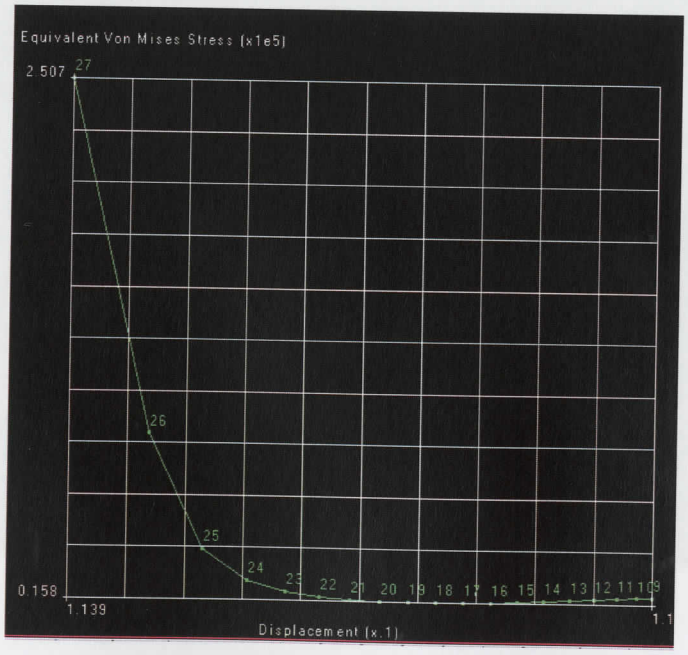

Figure 5.10: *Circular Indenter Analysis Results*

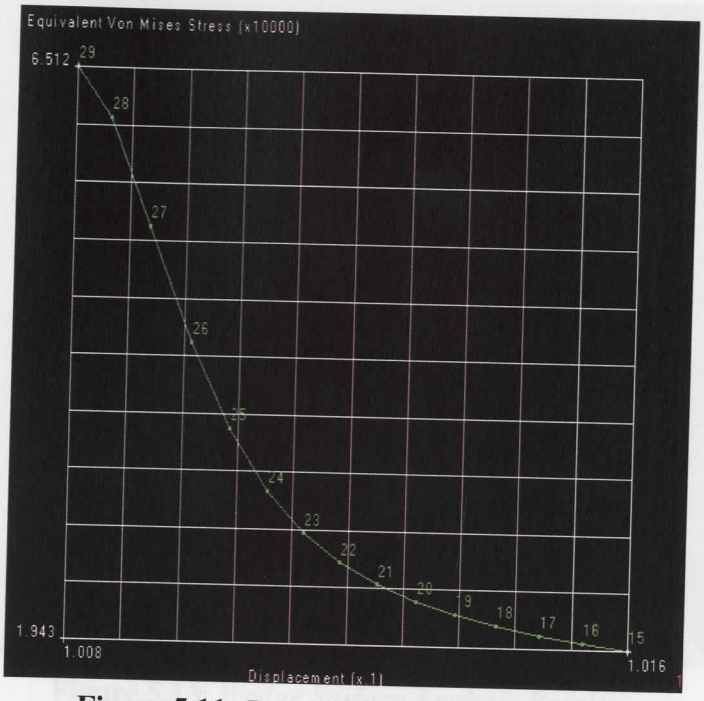

Figure 5.11: *Pyramidal Analysis Results*

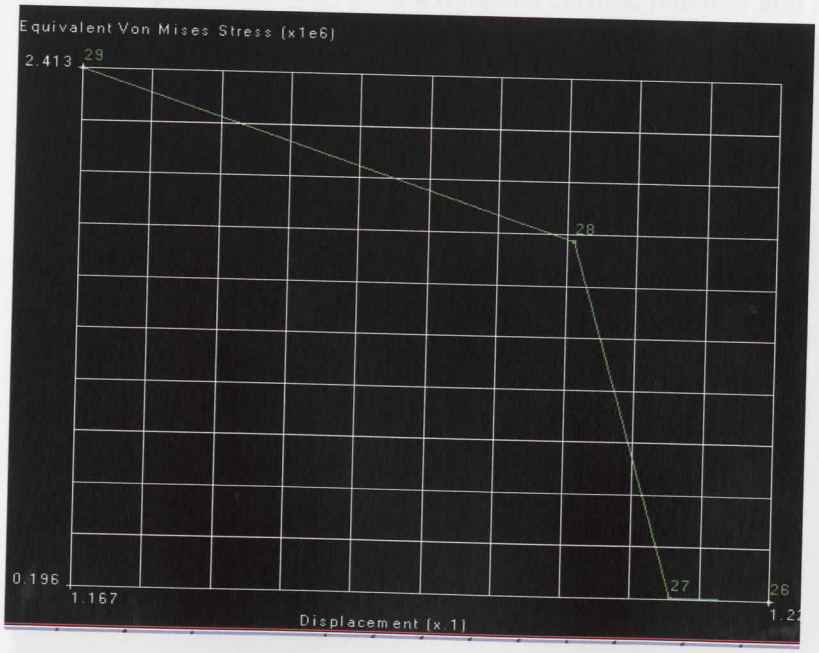

Figure 5.12: *Flat Surface Analysis Results*

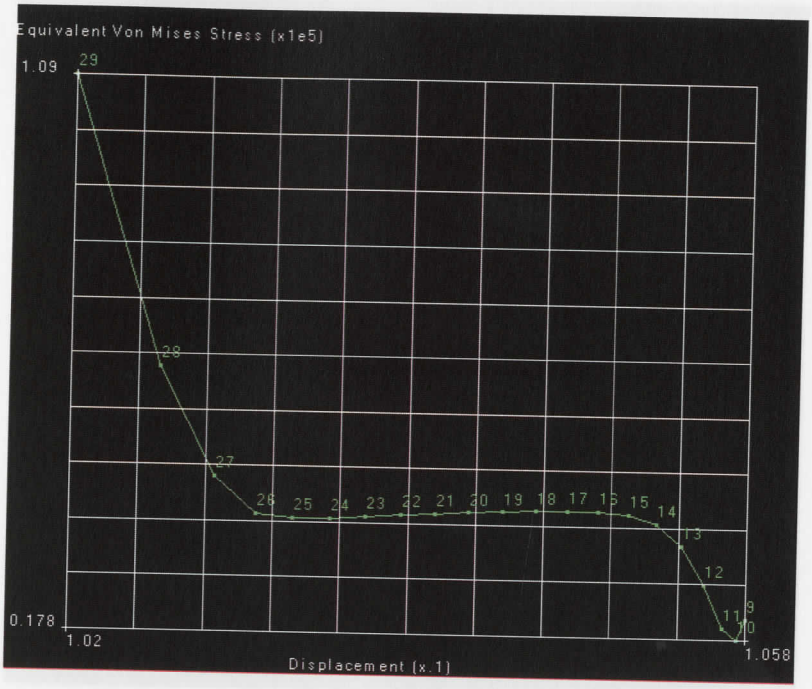

Figure 5.13: *Wedge Surface Analysis Results*

Case 2 Load displacement curves of a tungsten carbide indenter and a steel specimen

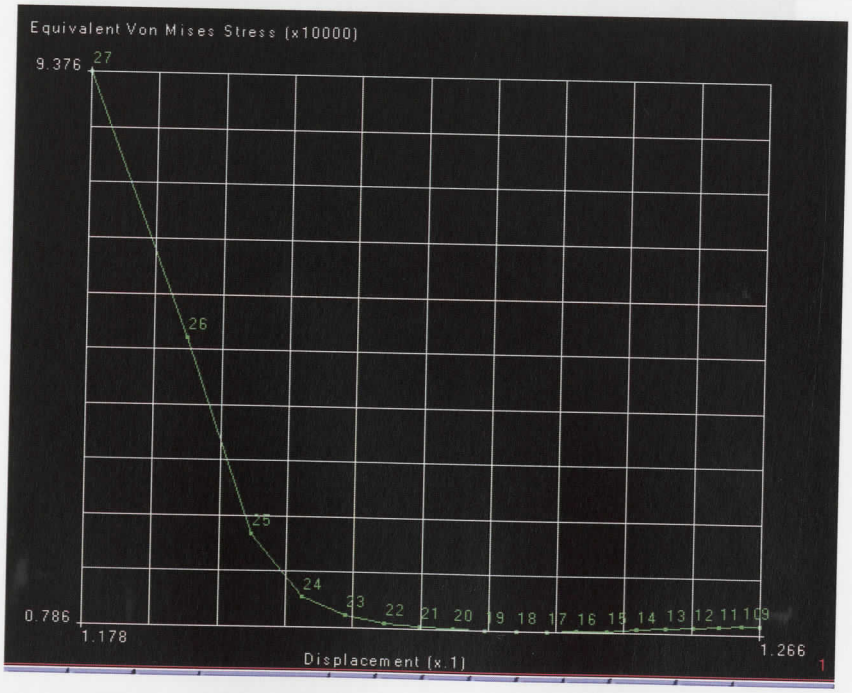

Figure 5.14: *Circular Indenter Analysis Results*

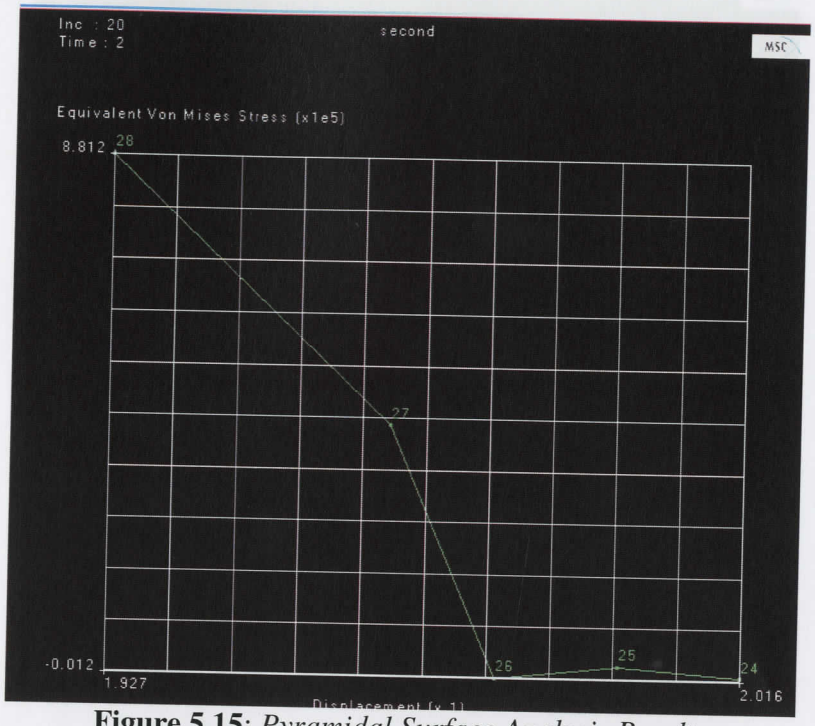

Figure 5.15: *Pyramidal Surface Analysis Results*

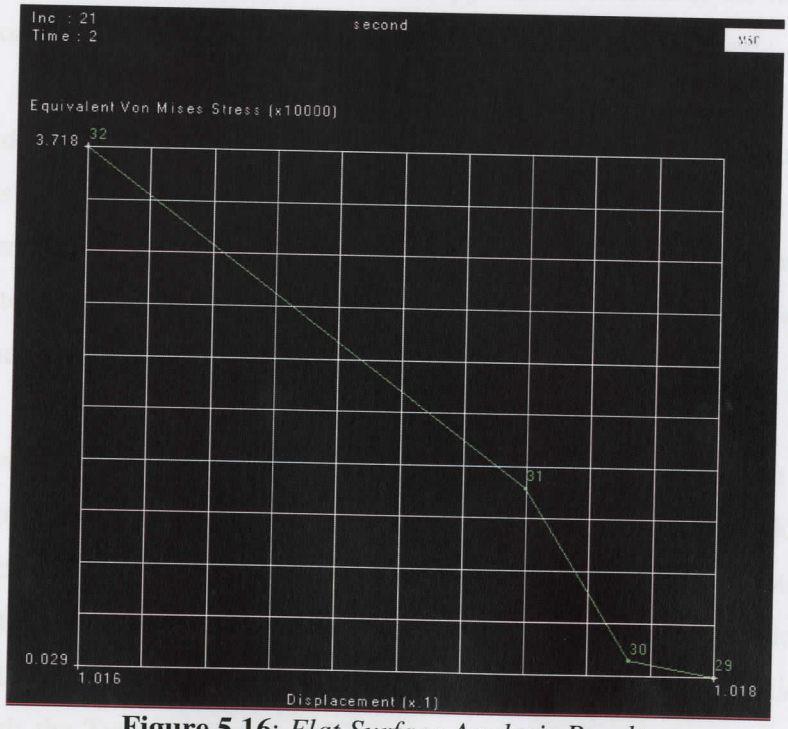

Figure 5.16: *Flat Surface Analysis Results*

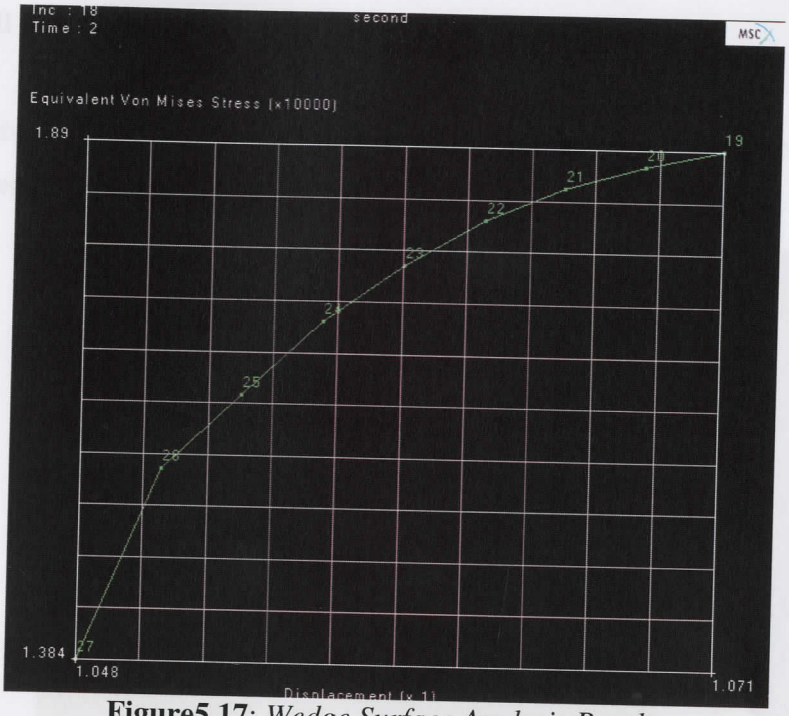

Figure5.17: *Wedge Surface Analysis Results*

When an indentation is formed by circular and pyramidal indenters, the material around the indentation is displaced and, in general the yield stress Y is increased. As the load on the indenter is increased, the amount of plastic deformation around the indentation increases and the mean pressure steadily rises until the whole material around the indentation is in a state of plasticity. Hence the maximum stresses occur at the tips of these indenters. It is not easy to define the stage at which this occurs, and the simple approach is to say that it is reached when the yield pressure varies little with further increase in indentation size.

It was observed that when these two metals are in contact the hydrostatic pressure will not of itself produce plastic deformation. The indenter, for which the yield stress under uni-axial stress is Y, is subjected to the hydrostatic pressure, it still require a superimposed uni-axial stress Y to produce plastic deformation. The plastic deformation occurs when the maximum shear stress reaches a certain critical value. This result is also consistent with the Tresca criterion, which suggests that plastic flow in general occurs when the maximum shear becomes equal to $\frac{1}{2}Y$.

5.1.5 Small Punch Results

For the results presented in figure 9 below circular tungsten carbide indenter was used on mild steel specimens.

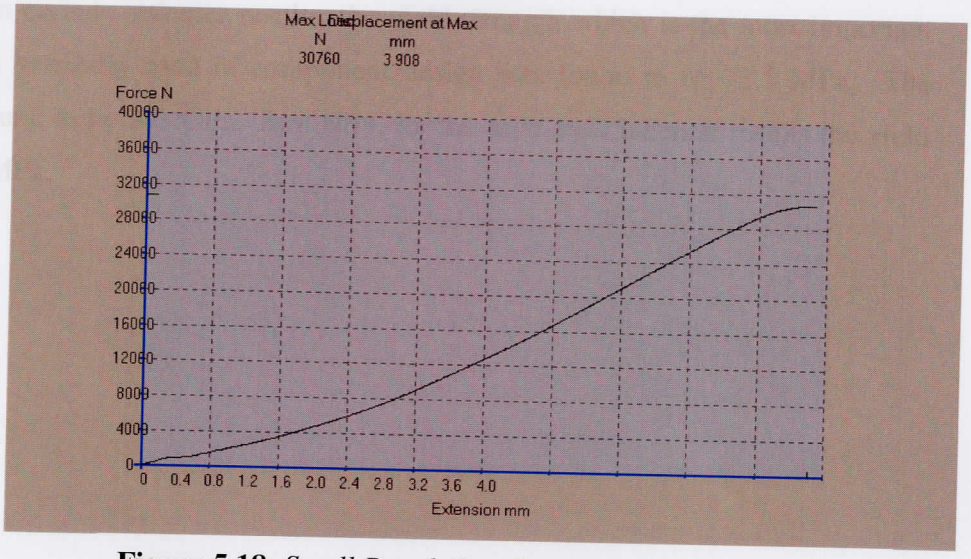

Figure 5.18: *Small Punch Test Data, load vs. displacement*

For the results presented in figure 5.19 below circular mild steel indenter was used on aluminium specimens.

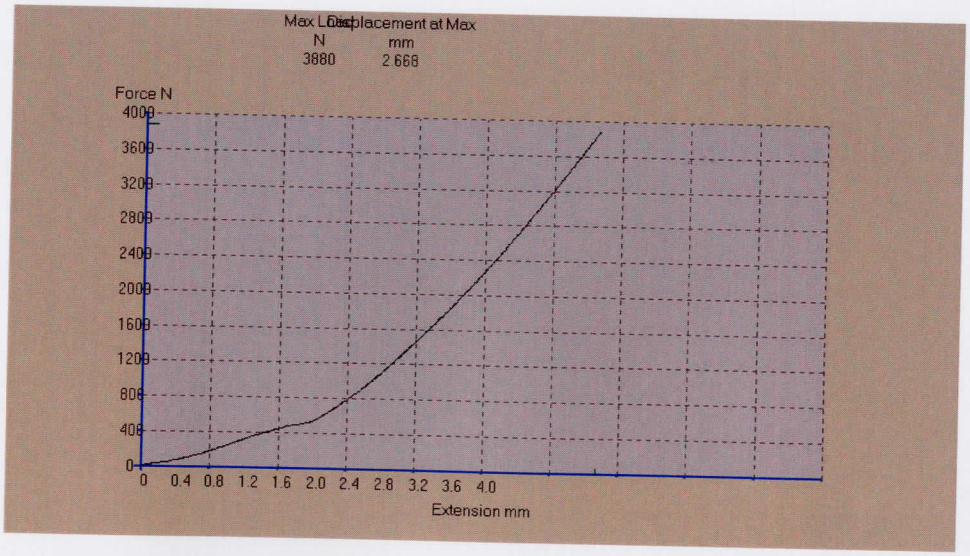

Figure 5.19: *Small Punch Test Data, load vs. displacement*

5.1.6 Discussion of the Small Punch Results

These significant results are used to deduce mechanical properties of material under the indenter. They show a direct proportion between the load and displacement parameters. For the tungsten carbide indenter results, the yield strength which is the most important property that is generally used in component design was found to be 77.5 MPa. The stiffness was found to be 203 GPa. Similarly, for the mild steel indenter results the yield stress is 4.875 MPa.

Chapter 6

Conclusions and Recommendations

6.1 Conclusions

This thesis was directed at manufacturing a Small Punch test for South African heavy industry as a means of determining mechanical properties of materials at different levels of degradation. The indentation method derived in this thesis for measurement of mechanical properties is not new. Small Punch testing is a growing field that incorporates fracture toughness, fatigue, thermal fatigue, fracture appearance and transition temperature (FATT), creep etc.

Shape sensitivity analysis using FEA was used to determine suitable shapes to be used for the Small Punch test. From the FEA results the circular and pyramidal indenters were found to be suitable for the indenter application in the Small Punch experiment (refer to figure 5.2 and 5.3 for the shapes.). The validation of these FEA results using the hardness test (ROCKLY HLN-11A) proved that these two indenters caused yielding or plastic flow easily. For circular and pyramidal indenter, the material displaced by the indenter was accommodated by the elastic-plastic expansion of the surrounding material. During this phase, the displacement of material was approximately radial from the point of first contact. The material displaced by the indenter piles up at the sides without any further increase in pressure.

The wedge and the flat surface indenters required a significant increase of the load or the edge pressure in order to cause plastic flow or yielding. Hence the wedge and the flat surface indenters were not chosen for indenter application.

The functionality of the Small Punch test was verified and can be used to determine mechanical properties at different levels of degradation. The objectives of the thesis were met and the results are summarised as follows:

(i) The Small Punch test indenter (6 mm diameter and 150 mm long), indenter holder (10 mm treaded diameter and 100mm long) and a specimen holder (250 mm x 200 mm with a 100 mm diameter and 50mm deep hole in the middle) were manufactured assembled and retrofitted into the University's existing tensile testing machine (See figure 4.2 for the illustration)

(ii) Small Punch and tensile tests were performed on 20 specimens of which 10 were mild steel and the other 10 were aluminium.

(iii) Small Punch load displacement curve gave similar results to the tensile test results in the elastic region of the material. The elastic moduli of both materials were determined and found to be 203 GPa and 68 GPa when using a Small Punch test or a tensile test on mild steel specimens and aluminium specimens respectively. Similarly, the yield stress was found to be 77.5 MPa and 4.875 MPa when using a Small Punch test or a tensile test on mild steel and aluminium specimens respectively.

(iv) In order to calculate all displacement curves up to the maximum load, it was necessary to consider a small friction effect between the indenter and the specimen. The friction effect is apparent only for displacement smaller than 0.8 mm and fades away as the load is increased.

The results obtained from the Small Punch test are similar to the Small Punch test results by Campitelli et al when they tested other ductile steel.

6.2 Recommendations

To date, the Small Punch Testing technique is not used world wide because the test results are not return in formats.

The future work should be focused on testing of materials of industrial choice at both ambient and elevated temperatures. Furthermore, focus should be on designing a small scale Small Punch which can be used as an on-line plant testing in collaboration with industry. The determination of fracture toughness, fatigue at ambient temperature and thermal fatigue at elevated temperatures will be the next step of this technological investigation.

This work can also on a larger scale be focused on creep studies as well as the estimation of remaining life in in-service components.

Bibliography

ASME Section XI 2001 ASME Boiler and Pressure Vessel Code, Section XI: Rules for In-service Inspection of Nuclear Power Plant Components American Society of Mechanical Engineers

Baik, J.-M., Kameda, J., Buck, O., 1983. **Small Punch test of intergranular embrittlement of an alloy steel. Scripta Metall**. 17, 1443–1447.

Bathe K.J. "**Finite Element Procedures in Engineering Analysis"** Prentice Hall, Europe, 1982. ISBN: 0-13-317305-4

Brinell J.A. (1900) "**Congrés International des Méthodes d'Essai"**, Paris

Bröklen R. (1971) "**A Simple Method for Obtaining the Ductility from a 100^0 Cone Impression**", The Science of Hardness Testing and its Research Applications. ASM.

Bulloch, J.H., 1998. **Toughness losses in low alloy steels at high temperatures: an appraisal of certain factors concerning the Small Punch test**. Int. J. Press. Vessels Piping 75, 791–804.

Campitelli E.N., Spa¨tig P., Bonade´ R, Hoffelner W., Victoria M. **Assessment of the constitutive properties from small ball punch test: experiment and** modeling Int. J. Press. Nuclear Materials 335, 370–371.

Davis H.E. Troxell G.E. & Wiskocil C.T. (1964) "**The Testing and Inspection of Engineering Materials**, McGraw-Hill Book Company

Desai C.S. and Siriwardane H.J **"Constitutive Law for Engineering Materials: With emphasis on Geologic Materials.** Prentice Hall, New Jersey, USA 1984. ISBN: 0-13-167940-6

Dobes F., Milicka K., On the Monkman–**Grant relation for Small Punch test data, Materials Science and Engineering** (A 336) 2002, pp 245–248.

Foulds J.R., Woytowitz P.J., Parnell T.K., Jewell C.W., **Fracture toughness by Small Punch testing, Journal of Testing and Evaluation,** JTEVA 23 (1) 1995, pp 3–10.

Fung Y.C. "**A First Course in Continuum Mechanics"**. 3rd edition, Prentice Hall, New Jersey, USA 1994. ISBN: 0-13-061524-2.

Harmer D.E, Troxell G.E., and Hauck G.W.F. "**The Testing of Engineering Materials"**, McGraw-Hill, New York, USA, fourth edition, 1982. ISBN: 0-07-015656-5.

Hill R. "**The Mathematical Model of Plasticity**" Clarendon, Oxford, UK, 1950, 1985, ISBN: 0-19-856162-8

Holzapfel G.A. "**Non Linear Solid Mechanics**" John Wiley and Sons, England, 2001. ISBN:

Joo, Y.-H., Hashida, T., Takahashi, H., 1992. **Determination of ductile–brittle transition temperature (DBTT) in dynamic Small Punch test.** J. Test. Eval. 20, 6–14.

Lipson C. (1967) "**Wear consideration in Design**", Prentice hall, Inc. N. j.

Logan D.L. "**A First Course in the Finite Element Method**". 2nd edition. PWS, Boston, 1993 ISBN: 0-534-92964-8

Ludwik P. (1908) "**Die Kegelprobe**", J. Springer, Berlin.

Manahan M.P., Browning A.E., Argon A.S., Harling O.K., Miniaturized Disk Bend Test Technique Development and Application, **The Use of Small-Scale Specimen for Testing Irradiated Material**, STP 888, American Society for Testing and Materials, Philadelphia, 1986, pp. 17-49

McNaney, J., Lucas, G.E., Odette, G.R., 1991. **Application of ball punch tests to evaluating fracture mode transition in ferritic steels**. J. Nucl. Mater. 179–181, 429–433.

Martel R. (1895) "**Commission des Méthodes d'Essai des Matériaux de Construction,** Paris 3, 261.

Mase G.T. and Mase G.E. "**Continuum Mechanics for Engineering**". 2nd edition, CRC Press, USA, 1999. ISBN 0-8493-1855-6

Meyer E. (1908) "**Zeits. d. Vereins Deutsch. Ingeniere**", 52, 645

Misawa, T., Adachi, T., Saito, M., Hamaguchi,Y., 1987. **Small Punch tests for evaluating ductile–brittle transition behavior of irradiated ferritic steels.** J. Nucl. Mater. 150, 194– 02.

Mohs F. (1822) "**Grundriss der Mineralogic,** Dresden.

Nadai A. "**Plasticity**", McGraw-Hill, New York

Nqabisa, S. (2003) **Thesis Submitted Towards a Bachelor of Technology Degree in Mechanical Engineering.** Peninsula Technikon South Africa (Cape Town)

O'Neill H. (1967) "**Hardness Measurement of Metals and Alloys.** 2nd edition Chapman and Hall Ltd. London

Patricia Han. **"Tensile Testing"**, 2nd edition. ASM International, USA, 1993 ISBN: 0-87170-440-4

Penny R.K. (1999) **"Ageing of Materials and Methods for the assessment of Lifetimes of Engineering Plant** Chameleon Press Ltd. London

Penny R.K (2005) "**Asset Management of Aged Plant and Materials: Assessment Methods** *Damage Mechanics, Extrapolation and Remaining Life Estimation,* March_2005 Eastbourne, England

Penny R.K. and Marriott D.L., "**Design for Creep**". 2nd edition. Chapman & Hall, London, 1995.

Penny R.K.(2001) and Kohlhöfer W., **Aging of Materials and Methods for the Assessment of Lifetimes of Engineering Plants**. *Proc. Cape '2001 Some Neglected NDT Tools,* April 2001 Elsevier, Oxford.

Penny R.K. (1995) **"The use of damage concepts in component life assessment"** *Proc. Cape '95. Ageing of Materials and life assessment*, March 1995 Elsevier, Oxford.

Shore A.F. (1918), "**Journal of Iron and Steel Inst."**, 2, 59. (Rebound Scleroscope).

South African standard which applies to test pieces taken from metallic products as specified in the relevant product standard.www.sabs.co.za

Tabor D. (1951) "**The Hardness of Metals"**, Claredon Press

Timing R. L. "**Engineering Materials**", 2nd edition Addison Wesley Longman Limited, Europe, 1998. ISBN: 0-582-31928-5.

Tonge, B.Y. **"The intermediate beam: theory and examples"** Butterworth's, London, 1972. ISBN: 0408702982

Zienkiewics O.C. "**The Finite Element Method"** 4th edition. McGraw-Hill, Europe, 1994. ISBN: 0-07-084174-8

Appendix A

Material Data

IN THIS APPENDIX some standard properties of mild steel and aluminium used in the experiments described in chapter 4 are presented.

A.1 Steel Properties

Material Name: Mild Steel

Manufacturer: Mac Steel

Physical Properties:

Property	Symbol	Value	Unit
Density	ρ	7850	kg/m^3
Young's Modulus	E	210	GPa
Shear Modulus	G	810	GPa
Poisson ratio	υ	0.3	——

Mechanical Properties:

Property	Symbol	Value	Unit
Yield Limit (min)	R_{eH}	355	MPa
Tensile Strength (min-max)	R_m	430-550	MPa

A.2 Aluminium Properties

Material Name: Aluminium

Manufacturer: Mac Steel

Physical Properties:

Property	Symbol	Value	Unit
Density	ρ	2700	kg/m^3
Young's Modulus	E	70	GPa

Shear Modulus	G	26	GPa
Poisson ratio	υ	0.33	——

Mechanical Properties:

Property	Symbol	Value	Unit
Yield Limit (min)	R_{eH}	49	MPa
Tensile Strength	R_m	90	MPa

A.3 Tensile Test Data

The data presented here is a plot of true (Cauchy) stress versus true (logarithmic) strain in figure A.1 below

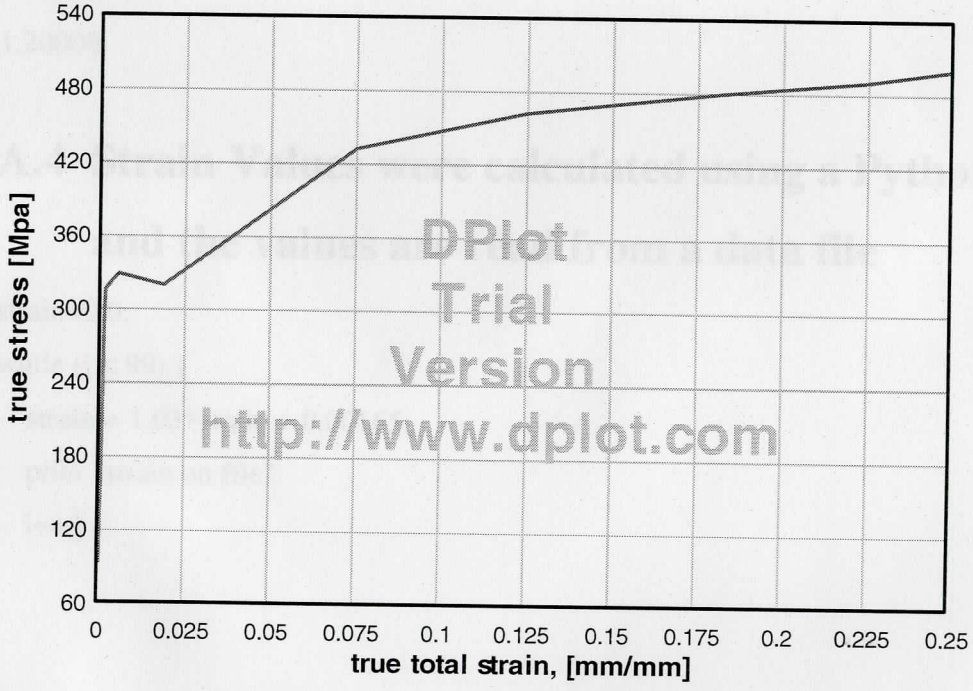

Figure A.1: *Tensile test Data, true stress versus true strain*

A.4 Strain Data

The strain values were distributed over a range of 0% to 120% strain with 10 points.

0.00000

0.00420

0.00850

0.01500

0.03500

0.05500

0.09500

0.15000

0.55000

1.20000

A.4 Strain Values were calculated using a Python code and the values are read from a data file

```
strain=0.0;
while (i < 99) {
   strain = 1.03*strain + 0.00165;
   print "strain on file"
   i++}
```